Cellular and Molecular Bioengineering, Vol. 4, No. 4, December 2011 *(© 2011)* pp. 510–537
DOI: 10.1007/s12195-011-0179-6

An Integrative Review of Mechanotransduction in Endothelial, Epithelial (Renal) and Dendritic Cells (Osteocytes)

SHELDON WEINBAUM,[1] YI DUAN,[2] MIA M. THI,[3] and LIDAN YOU[4]

[1]Department of Biomedical Engineering, The City College of the City University of New York, New York, NY 10031, USA; [2]Center for Advanced Research and Technology, Kinetic Concepts, Inc., Branchburg, NJ 08876, USA; [3]Department of Orthopaedic Surgery and Dominick P. Purpura Department of Neuroscience, Albert Einstein College of Medicine of Yeshiva University, Bronx, NY 10461, USA; and [4]Department of Mechanical and Industrial Engineering, Institute of Biomaterials and Biomedical Engineering, University of Toronto, Toronto, ON, Canada

(Received 16 March 2011; accepted 20 May 2011; published online 4 June 2011)

Associate Editors John Shyy and Yingxiao Wang oversaw the review of this article.

Abstract—In this review we will examine from a biomechanical and ultrastructural viewpoint how the cytoskeletal specialization of three basic cell types, endothelial cells (ECs), epithelial cells (renal tubule) and dendritic cells (osteocytes), enables the mechano-sensing of fluid flow in both their native *in vivo* environment and in culture, and the downstream signaling that is initiated at the molecular level in response to fluid flow. These cellular responses will be discussed in terms of basic mysteries and paradoxes encountered by each cell type. In ECs fluid shear stress (FSS) is nearly entirely attenuated by the endothelial glycocalyx that covers their apical membrane and yet FSS is communicated to both intracellular and junctional molecular components in activating a wide variety of signaling pathways. The same is true in proximal tubule (PT) cells where a dense brush border of microvilli covers the apical surface and the flow at the apical membrane is negligible. A four decade old unexplained mystery is the ability of PT epithelia to reliably reabsorb 60% of the flow entering the tubule regardless of the glomerular filtration rate. In the cortical collecting duct (CCD) the flow rates are so low that a special sensing apparatus, a primary cilia is needed to detect very small variations in tubular flow. In bone it has been a century old mystery as to how osteocytes embedded in a stiff mineralized tissue are able to sense miniscule whole tissue strains that are far smaller than the cellular level strains required to activate osteocytes *in vitro*.

Keywords—Endothelial glycocalyx, Actin cortical web, Proximal tubule, Cortical collecting duct, Brush border microvilli, Lacunar-canalicular system, Actin filament bundles, Bone cell processes, Integrin attachments.

Address correspondence to Sheldon Weinbaum, Department of Biomedical Engineering, The City College of the City University of New York, 140 Convent Avenue, New York, NY 10031, USA. Electronic mail: weinbaum@ccny.cuny.edu

INTRODUCTION

It is indeed a pleasure for the senior author to submit a paper to this special issue of Cellular and Molecular Engineering on mechanobiology in honor of Dr. Shu Chien's 80th birthday. We first met in 1969 on the occasion of the 50th anniversary of the Grove School of Engineering at The City College through our mutual colleague, Dr. Yuan-Cheng Fung. In the summer of 1971 I audited a course that he directed at Columbia University School of Medicine for medical students on physiology and biophysics, and shortly thereafter we started a well-recognized scientific collaboration of over 30 years duration on endothelial aspects of atherogenesis and leukocyte rolling. In the past decade Dr. Chien has made pioneering contributions to the molecular signaling initiated by fluid shear stress (FSS) acting on vascular endothelial cells (ECs) including the activation of RhoA by integrins in the modulation of gene expression[142] and the development of a genetically encoded Src reporter that enabled the spatial-temporal tracking of Src in living HUVECS.[165] These insights have been pivotal to our understanding of how mechanical stimuli affect cellular functions such as apoptosis, migration and remodeling, and gene expression.[25,90]

In the present paper we will examine from a biomechanical and ultrastructural viewpoint how the cytoskeletal specialization of three basic cell types, ECs, epithelial cells (renal tubule) and dendritic cells (osteocytes), enables the mechano-sensing of fluid flow in their native *in vivo* environment. FSS is the mechanical stimulus that leads to the molecular activation and cellular regulation in Dr. Chien's *in vitro* studies on ECs. There have been detailed recent reviews on the fluid flow and mechanobiology for each

of these three cell types: ECs,[175] renal epithelia[118,173]; bone cells.[53,75] The purpose of the present paper is not to summarize these reviews, but to provide an integrative and comparative analysis of the structure and function of the mechanosensing organelles for fluid flow for all three cell types. With this goal in mind I have invited three former PhD students, who have contributed greatly to our understanding of mechanotransduction in each cell type, to be co-authors of this integrative study.

All cells that sense fluid flow have special sensory organelles that are specific to their local mechanical environment and the regulatory functions that they must serve. In the last decade there has been an explosion of interest in mechanobiology at the cellular and molecular level. This is summarized in a recent white paper, Discher *et al.*,[34] and the cover article on mechanobiology in *The Scientist*.[4] As stated in the white paper "in order to understand key aspects of health and disease we must first be able to explain how physical forces and mechanical structures contribute to the active material properties of living cells and tissues, as well as how these forces impact information processing and cellular decision making." Mechanobiology has many aspects from the interaction of the cell with its substrate or scaffold,[35,42] to the application of the mechanical forces and their measurement,[44,66,71,143,164] to the cytoskeletal and molecular reorganization that results from their application.[40,159] In this paper we shall focus primarily on the specialized structures that exist on the apical surfaces of cells and/or their surrounding matrix that enables them to detect fluid forces, amplify these mechanical signals, transmit them into the cell's intracellular cytoskeleton, and the downstream signaling that results.

BASIC MYSTERIES AND PARADOXES

Endothelial Cells (ECs)

In the case of ECs it had been widely recognized since the early electronmicroscopic studies of Luft[95] that the endothelial surface was coated with a glycocalyx of proteoglycans and glycoproteins. However, relatively little attention was paid to this endothelial glycocalyx layer (EGL) until the pioneering paper of Vink and Duling[163] clearly demonstrated in hamster microvessels *in vivo* that this layer played a vital role in the hematocrit distribution of the microcirculation. Subsequently, Michel[105] and Weinbaum[171] proposed that this layer also served as the molecular sieve for plasma proteins and that the classical Starling forces for the oncotic pressure had to be applied locally across this layer as opposed to the global difference between plasma and tissue as had been widely assumed since Starling's[145] groundbreaking paper on microvascular fluid exchange. Theoretical models clearly predicted that FSS was greatly attenuated by this layer and that the actual FSS at the apical membrane of the ECs was negligible.[29,47,140] This raised a fundamental paradox, how was FSS transmitted across the plasma membrane into the intracellular cytoskeleton of the ECs if the FSS at the apical membrane vanished. The widely used diagram for intracellular signaling in Davies,[31] which neglected the EGL, was clearly incomplete. The potential role of the EGL in mechanotransduction was first suggested in Secomb *et al.*[140] Subsequently, Weinbaum *et al.*[176] proposed an ultrastructurally based elastohydrodynamic model in which it was suggested that the heparan sulfate proteoglycans in the EGL were anchored into the actin cortical web (ACW) beneath the plasmalemma of the ECs and that the bending moment on these core proteins due to the FSS acting at the edge of the EGL was transmitted across the apical membrane into the ACW due to their flexural rigidity EI, where E is Young's modulus and I is the moment of the inertia of the cross section. This ultrastructural model was based on the electron-microscopic observations in Squire *et al.*[144] These studies, alternative views of the EGL and more recent developments are described in two review papers on the structure and function of the EGL.[155,175]

Epithelial Cells (Renal Tubule)

Aside from hair cells in the inner ear, the most widely studied application of mechanotransduction in epithelial cells is the fluid flow in the proximal tubule (PT) and cortical collecting duct (CCD) of the renal tubule. In the PT a four decade old mystery was the afferent mechanism in glomerulo-tubular balance (GTB), the ability of brush border epithelial cells in the PT to reliably absorb roughly 2/3 of the filtered load over a wide range of glomerular filtration rates (GFR) that could vary from 5 to 50 nl/min in humans.[137] A second equally important puzzle was the fact that FSS in the PT, typically 1 dyn/cm^2, was an order of magnitude less than in ECs,[61] even for higher GFR. At these low values of FSS there was little if any intracellular biochemical response in ECs. In the CCD, the FSS was further reduced by a factor of five and yet the principal cells of the CCD were able to detect such very low fluid flow rates and elicit a biochemical response, the opening of Ca^{2+} ion channels that led to the release of Ca^{2+} from intracellular stores.[116] It was clear that in both cases highly specialized cellular structures were required to greatly amplify hydrodynamic forces in contrast to ECs where physiological levels of FSS, typically >10 dyn/cm^2, were sufficient to elicit intracellular signaling *in vitro*. A resolution to this

paradoxical behavior in the PT was proposed in Guo *et al.*[61] who suggested that the flow sensors in the brush border cells were the numerous microvilli (4000/cell) at the luminal surface and that the bending moment produced by the FSS at the tips of the closely spaced slender microvilli led to a 40-fold increase in force and stress concentration at the base of the microvilli at their insertion into the ACW of the epithelial cells.[174] For the CCD Schwartz *et al.*[138] proposed and Praetorius and Spring[116] demonstrated that 9 + 0 non motile primary cilia (PC) were the activating organelle for the initial influx of Ca^{2+}. These and more recent developments are described in a recent review paper on mechanotransduction in the renal tubule.[173]

Dendritic Cells (Osteocytes)

It was recognized more than a century ago that the trabecular structure of bone was closely related to its mechanical loading, often referred to as Wolff's Law. The mystery was how the mechanical loading of bone was sensed by the cells, osteocytes, that lived in the mineralized bone matrix. These cells have the ability to detect very small strains due to human and animal locomotion which experiments indicate rarely exceed 1000 μstrain[52] with maximum strains during heavy exercise being 0.2%.[17] These mechanical signals are converted to intracellular biochemical signals and then communicated to osteoblasts at the bone surface to produce new bone or osteoclasts at the bone surface to resorb old bone. A second paradox is the fact that these small whole tissue strains are an order of magnitude smaller than the strains required to produce biochemical responses in bone cells in culture.[184] Early *in vitro* experiments on bone cells[126] had shown that osteoblast like cells in culture could elicit biochemical responses similar to ECs when exposed FSS in the same range as vascular endothelium. Piekarski and Munro[113] had shown that small whole bone deformations could lead to fluid movement in the interconnected lacunar-canalicular network. This network was largely studied as a fluid flow conduit system to provide nutrients and remove wastes. The pericellular matrix surrounding the osteocytes with their long dendritic processes was ignored as well as the potential role of this matrix as a mechanotransducer. A turning point was the theoretical paper by Weinbaum *et al.*[172] which predicted, contrary to intuition, that the FSS on the slender dendritic processes due to the fluid flow through the pericellular matrix in the narrow canaliculi was comparable to the FSS on ECs in our vascular system. Using a new technique to isolate osteocytes from bone tissue, Klein-Nulend *et al.*[78] were able to demonstrate the sensitivity of osteocytes to FSS at the levels predicted by Weinbaum *et al.*[172]

While it is now generally accepted that fluid flow is sensed by osteocytes in living bone, the actual mechanism is still being actively debated. You *et al.*[180] proposed that it is not the FSS on the dendritic processes that is the source of the mechanical signal, but rather the fluid drag on the tethering matrix elements that attach the processes to the canalicular wall. Experiments by You *et al.*[183] confirmed the existence of these tethering elements and also provided detailed ultrastructural data for the organization of the cell process. Han *et al.*[63] then used this data to construct a refined biomechanical model which showed that whole tissue strains could be amplified by at least an order of magnitude at the cellular level by the tension in the tethering fibers produced by the fluid drag on the pericellular matrix. Such behavior would explain the second paradox as to how whole tissue strains could be greatly amplified at the cellular level. Several recent papers have suggested alternative mechanisms for osteocyte mechanotransduction. Wang *et al.*[170] and McNamara *et al.*[104] propose that in addition to the flexible tethering filaments there are more rigid integrin attachments at discrete sites along the canalicular wall where collagen fibrils create local regions of near contact with the cell processes. Wang *et al.*[170] predicts that these sites serve as local stress and strain concentrators that lead to the opening of stretch activated ion channels. Another mechanism proposed by Malone *et al.*[98] is that non motile primary cilia observed on bone cells in culture and osteocytes in newly formed bone[45] could also serve as mechanosensors of fluid flow. These various possibilities are described in greater detail in two recent review papers.[53,75]

Each of the following sections will be divided into three parts, one for each cell type like the present section on Basic Mysteries and Paradoxes.

ULTRASTRUCTURAL MODELS

Endothelial Cells

The EGL is a remarkable layer with multifaceted roles; it functions as a molecular sieve for plasma proteins,[105,163] as a barrier that modulates hemodynamic interaction between red blood cells and leukocytes[47,139,161,187] and ECs and as a mechanotransducer of FSS.[140] A fundamental question that arises is what kind of ultrastructure could adapt and perform these multiple functions? Luft[95] first identified the existence of the EGL in the 1960s using ruthenium red staining. More recent electron-microscopic studies[20,161] show

hair-like protrusion structures that line the luminal surface of ECs as shown in Figs. 1a and 1b. The thickness of the EGL differs across various species; in mouse, rat, frog and hamster it varies between 100 and 500 nm[56,175] whereas in bovine and human ECs two recent studies suggest a thickness of 2–9 μm.[14,146] This wide disparity in thickness has yet to be explained. The integrity of this layer depends on the presence of plasma proteins.[2] The EGL is composed mainly of glycoproteins, sulfated proteoglycans, hyaluronic acid, sialic acids, and plasma proteins. Heparan sulfate (HS) is the most abundant proteoglycan in the EGL (~50–90%)[73,154] and generally co-expresses with the second most abundant proteoglycan, chondroitin sulfate (CS), in a ratio of 4:1.[67,125] Additional studies indicate that the transmembrane protein syndecan-4, a member of the HS family of proteoglycans, is linked to the actin cytoskeleton through actin-binding proteins[11,73] providing the direct association between the EGL and the underlying cytoskeleton for mechanotransduction. In addition, studies have shown that high glucose associated with diabetes as well as inflammation and ischemia induced shedding of the EGL.[107,109] The ultrastructural organization of the EGL was largely a mystery until the study by Squire and coworkers[144] using computed autocorrelation functions and Fourier transforms on the EGL samples obtained from various electron microscopic techniques showed that this layer was a quasi-periodic bush-like structure that appears to stem from the underlying ACW. The tangential view of freeze-fracture replicas and sagittal view from these computer-enhanced images of frog mesenteric capillary EGL showed evidence of a characteristic spacing of 20 nm in all directions as well as a well defined hexagonal lattice with anchoring foci periodically occurring at 100 nm spacing (Figs. 1c and 1e). Similar spacing has also been observed in the bush-like structures of the EGL emanating from a common cluster that was close to the EC surface by Rostgaard and Qvortrup.[131] Based on these findings Squire *et al.*,[144] proposed an ultrastructural model for the EGL with the basic organization of the bush-like core protein structure and its connection to the underlying ACW with the spacing of different components as shown in Figs. 1d and 1f.

Renal Epithelial Cells

As mentioned in the previous section, FSS in the renal PT is only 1/10 of that exposed to ECs. In order to perform the highly modulated GTB, special sensing machinery is needed for these cells to (1) sense variations in luminal FSS and (2) convert these mechanical signals into membrane transporter activities, which in turn lead to physiological responses. In fact PT cells contain a highly architecturally and functionally specialized apical domain, i.e. brush border (BB). Freeze fracture study has revealed that microvilli (MV), numerous finger-like protrusions of brush border, are strikingly uniform in height (Fig. 2A)[111] and tightly packed in an exquisite, well-ordered hexagonal pattern.[99] Ultrastructurally brush border microvilli (BBMV) in proximal tubule cells share similar components with intestinal cells (Fig. 2B). They both are generally short (1–5 μm in height) and about 0.1 μm in diameter. Each microvillus contains a central actin filament bundle, which is associated with the actin-bundling proteins villin, fimbrin, and espin,[10,130] and is linked to the plasma membrane by a periodically spaced spiral array of bridges composed of the class I myosin, myosin IA.[27] Villin and fimbrin have been found in the microvillar core, whereas myosin and spectrin appear in the terminal web.[130] Functionally, however, the BBMV in the small intestine and the PT differ greatly. The BBMV of the intestinal cells are essentially shielded from the flow, which makes them unlikely to be mechanosensors. Recently, these MV have been suggested to be important for the gut defense by releasing vesicles that are rich in intestinal alkaline phosphatase from their distal tips.[12,58,100] In contrast, the BBMV of the PTs are not only directly exposed to luminal flow, but are also considered to be a more rigid structure with numerous clathrin coated pits at its base.[130] Membrane linking proteins including members of the ezrin, radixin, and moesin superfamily[46] organize the membrane domains through their ability to interact with transmembrane proteins and the cytoskeleton. These traits make BBMV in the PTs a good candidate for mechanosensing.

The CCD is the final component of the renal tubule to influence the body's electrolyte and fluid balance. At times of extreme dehydration, one-quarter of the filtered water may be absorbed in CCD. How can cells in the CCD sense such minimal variations in flow and respond with biochemical changes? A structure that is both highly elongated and projects into the flow field is needed to amplify the mechanical signal. Primary cilia in the principle cells are such a structure. Located at the center of the cell's apical membrane, this microtubule-based nonmotile structure protrudes 2–3 μm[132] from its basal body into the luminal flow region and extends downward to connect with the actin cortical cytoskeleton, which in turn, links to the remainder of the deeper cytoskeleton in the underlying cytoplasm (composed of microfilaments, microtubules, and intermediate filaments).[74] Motor proteins (kinesins and dyneins) transport 'cargo' proteins up and down the microtubule 'rail' (Fig. 2C).

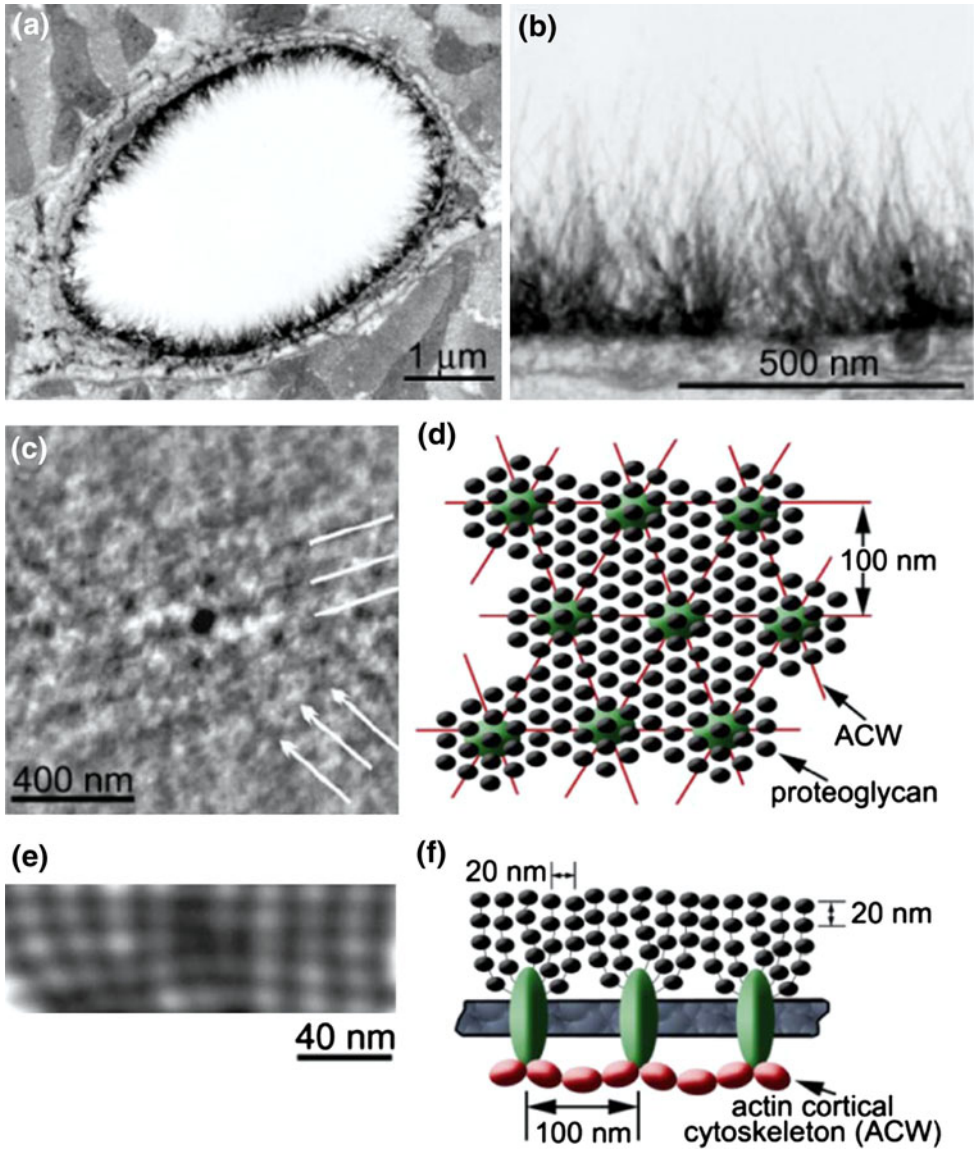

FIGURE 1. Ultrastructure of the endothelial glycocalyx layer (EGL). (a) An overview of transmission electron microscopy (TEM) image of a rat left ventricular myocardial capillary stained with Alcian blue (Bar = 1 μm). (b) A detailed image from (a) showing the distribution of hairy-like bushes in the EGL (Bar = 500 nm). (c) The computer-enhanced freeze-fracture image taken from the tangential inner surface of untreated frog mesenteric EGL showing a distinct quasi-hexagonal spacing around 100 nm (Bar = 400 nm). (d) Ultrastructural model of an EGL in tangential view. (e) An example of computer-enhanced sagittal section of the EGL with smaller periodic spacing approximately 20 nm (Bar = 40 nm). (f) The proposed ultrastructural model of an EGL in sagittal view showing the bush-like structure (glycoproteins) emanating from a common core protein cluster and its linkage to the underlying actin cortical cytoskeleton (ACW). From van den Berg *et al.*[161] and Squire *et al.*[144]

Dendritic Cells (Osteocytes)

Osteocytes are bone cells embedded in the mineralized matrix in bone. They are widely believed to be responsible for sensing the mechanical load applied on bone and coordinating bone turnover to meet the mechanical needs of its functional environment. The ultrastructure of the pericellular environment and intracellular components provide the key to understanding (1) how the tissue level loading is converted and amplified into cellular level mechanical stimuli; and (2) how these cellular level mechanical stimuli are translated into biochemical signals.

Bone matrix, although it appears as a rigid solid, is actually an interstitial fluid filled porous structure with 3 levels of porosity: (1) the vascular porosity (order 20–40 μm) which contains blood vessels and nerves[28]; (2) the lacunar-canalicular porosity (pericellular space order 100–1000 nm),[183] an interconnected system

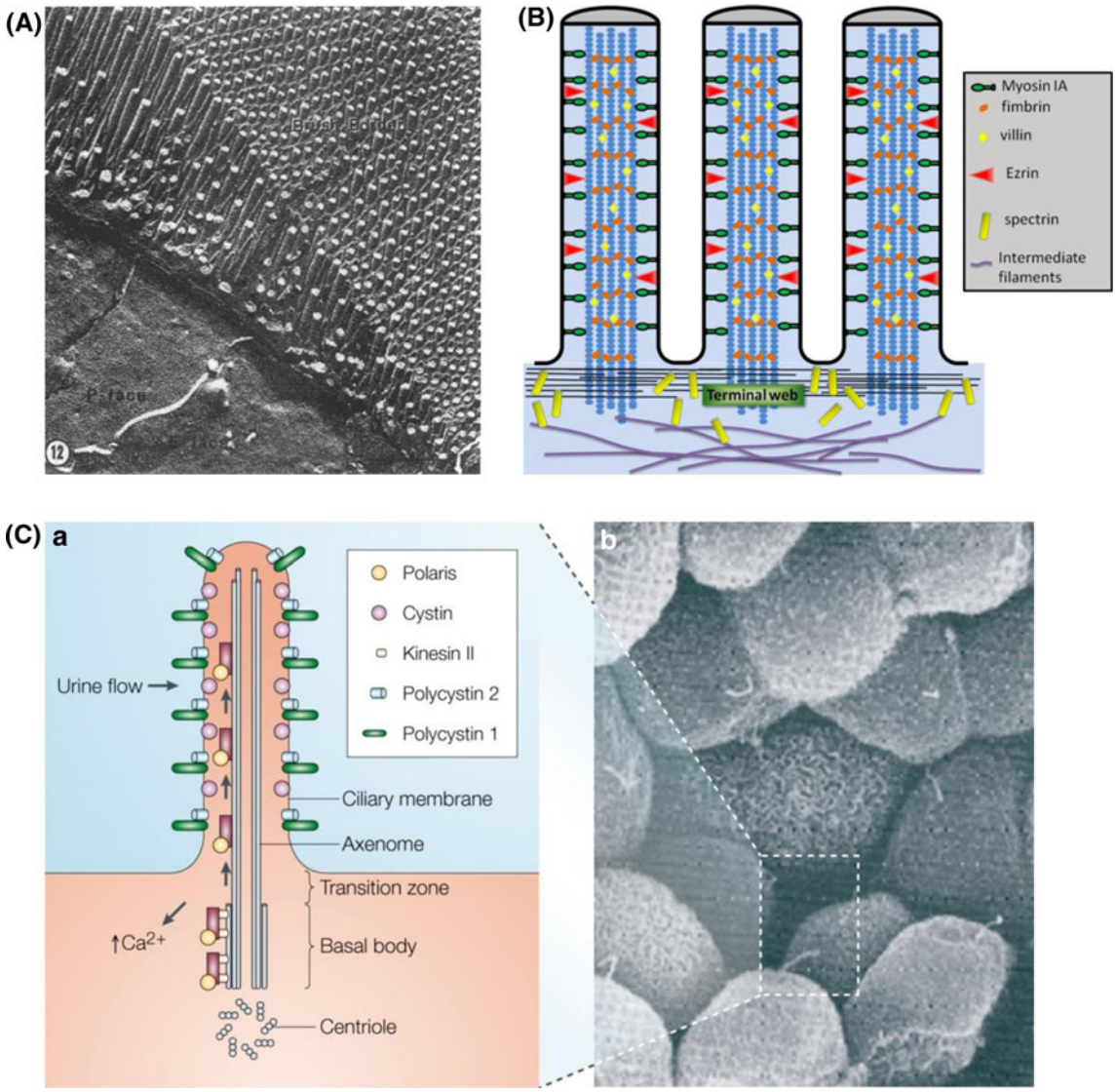

FIGURE 2. (A) Freeze-fracture appearance of the apical pole of a PT epithelial cell with its brush border. From Orci *et al.*[111] (B) Sketch of cytoskeleton inside an intestinal microvillus. The intracellular structure of the intestinal microvillus is composed of two regions, a brush border and a terminal web. Adapted from Weinbaum *et al.*[174] (C) In the primary cilium (a) of renal epithelial cells (b), 'cargo' proteins are trafficked along the microtubule tracks from the Golgi apparatus stack to the tip of the cilia using the motor protein kinesin II and back down using the cytoplasmic dynein1b (not shown). Adapted by permission from Macmillan Publishers Ltd: Nature Reviews Genetics,[69] copyright (2005).

which contains osteocyte bodies (lacunae) and processes (canaliculi); and (3) the collagen-apatite porosity (on the order of 2 nm).[28] Mechanical loading on bone has been proposed to induce the dynamic flow of the pericellular interstitial fluid in the lacunar-canalicular system (LCS).[113,172] Such a flow is believed to contribute greatly to osteocyte mechanotransduction.[16,172]

Between the osteocyte membrane and bone's mineralized matrix is a pericellular space filled with interstitial fluid and pericellular matrix. The width of this space between the osteocyte body and it's lacunae wall is typically 1 μm,[183] and the space between the osteocyte process membrane and the canalicular wall is on average 80 nm.[183] The nature of the pericellular matrix is not fully understood. Tracer studies have shown that the size of the pericellular matrix pores is roughly 7 nm. Electron microscopy studies have revealed the existence of tethering molecules in the pericellular matrix connecting the cell membrane to the surrounding canalicular wall (Fig. 3a).[183] Recently, Wang *et al.*[170] and McNamara *et al.*[104] have demonstrated that focal near contact attachments appear

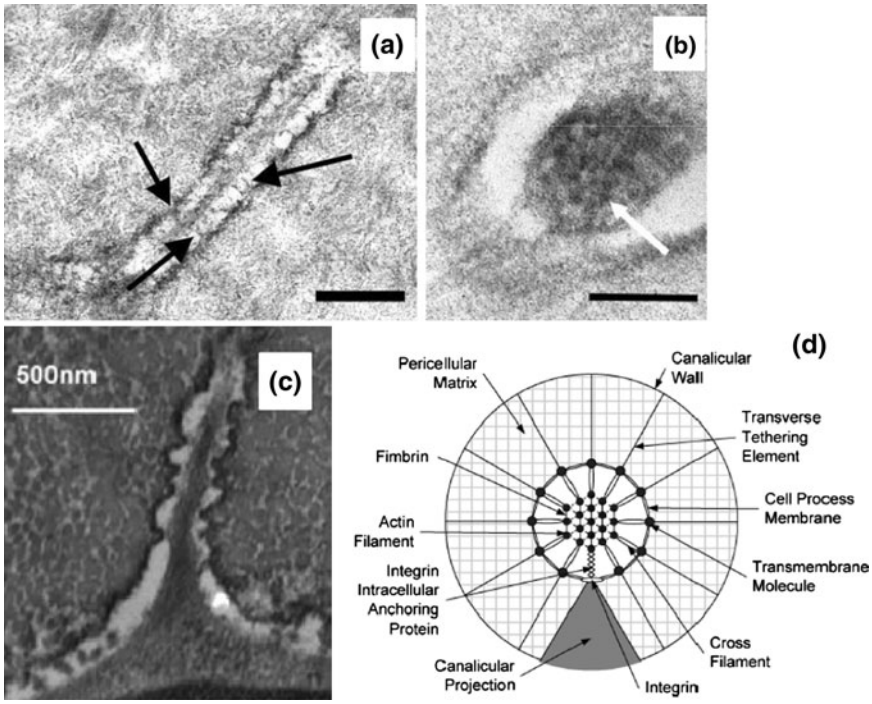

FIGURE 3. Ultrastructure of osteocyte process. (a) TEM photomicrograph showing the longitudinal section of an osteocyte process. Numerous transverse elements (arrows) can be seen extending from the cell process to the bony wall. Bar = 300 nm. From You *et al.*[183] (b) TEM photomicrograph showing a cross section of an osteocyte process. Darkened circular spots (see arrow) are cross sections of cytoskeletal filaments around 6–8 nm in diameter, consistent with the size of F-actin filaments. Bar = 100 nm From You *et al.*[183] (c) TEM photomicrograph of osteocyte shows longitudinal-sections of cell process showing that the bony wall of the canaliculus has protrusions projecting from the wall across the pericellular space in near contact with the cell membrane of the osteocyte process. From McNamara *et al.*[104] (d) Transverse cross-section of the idealized structural model for an osteocyte process in a canaliculus attached to a focal attachment complex and tethered by the pericellular matrix. From Wang *et al.*[170]

periodically along the osteocyte process which allow the canalicular wall to come in close apposition with the process membrane (Fig. 3c). Immunostaining studies demonstrate the existence of CD44,[110] and $\alpha_v\beta_3$ integrin[102] in the matrix surrounding the osteocyte process, suggesting that potentially CD44 serves as the tethering molecule, and the integrin serves as a focal attachment. Intracellularly, there is an hexagonally packed F-actin filament bundle with F-actin filaments cross-linked by fimbrin (Fig. 3b),[183] suggesting that the osteocyte process is much stiffer than the cell body. Interestingly, it has been found that primary cilia exist on the surface of osteocyte body cell membrane,[45,98] with length ranging from 2 to 9 μm, suggesting that it is packed tightly into the osteocyte cell body pericellular space (~1 μm). Recently, McNamara *et al.*[103] showed that primary cilia are present on osteocytes that reside within 25 μm of the periostial surface, but are entirely absent from deeper regions of the cortex of adult mouse cortical bone. This interesting finding suggests that primary cilia may be a signaling organelle that serves as a chemical sensor rather than as a mechanical sensor in osteocytes.

FLUID FLOW MODELS AND THEIR PREDICTIONS

Endothelial Cells

Three different models, oncotic, elasto-hydrodynamic, and electrochemical have been proposed for the restoring forces that provide for the structural integrity of the EGL and the maintenance of its thickness under FSS. The oncotic model, which assumed that an osmotic swelling force due to trapped proteins in the EGL provided for its structural integrity, was first proposed by Pries *et al.*[122] in their simulation of blood flow through vessel segments of large microvascular networks. These early models, which were largely concerned with the effect of the EGL on the hematocrit distribution and flow resistance in microvessels, are summarized in Pries *et al.*[121] Using biphasic theory for fluid flow through the EGL and axisymmetric theory for the flow of deformable red blood cells (RBCs) in narrow tubes, these models predicted a parachute shape for the RBCs, a substantial increase in flow resistance, and reduced capillary tube hematocrit due

to the EGL.[29,139] While treating the deformation of the RBCs, these models assumed the RBCs did not enter the EGL, in contrast to the observations of Vink and Duling[163] which showed that the RBCs both entered the EGL at low speeds (<20 μm/s) and exhibited a striking "pop-out" phenomenon when the RBCs started from rest. The latter behavior was first examined in Feng and Weinbaum[47] using a generalized lubrication theory for highly compressible porous media. The theory showed that the RBCs actually skied on the EGL, that the lift forces generated scaled as h^2/K_p, where h was the layer thickness and K_p the Darcy permeability, and the enhancement in lift due to the fiber layer could be four-orders-of magnitude greater than predicted by classical lubrication theory if there was no lateral leakage of pressure when the RBCs were completely surrounded by the capillary wall. A similar behavior was predicted by Secomb and coworkers[140,141] except that the restorative force of the layer after the RBCs passed was still attributed to a weak oncotic pressure. Subsequent models[3,72,185,186] for the oncotic force due to plasma proteins in the EGL clearly showed that the EGL served as a molecular sieve and that the oncotic forces within the layer were significantly lower than in the lumen of the vessel. These predictions led to a major revision of the century old Starling hypothesis, which had neglected the EGL.

In the absence of an appropriate oncotic force, two other models were proposed to explain why the EGL did not appear to change its thickness under FSS,[163] a linear elasto-hydrodynamic model[176] and an electrochemical model.[30] Weinbaum *et al.*[176] proposed that the structural integrity derived from the flexural rigidity EI of the core proteins in the layer and that the value of EI could be determined from the time constant observed in the preliminary experiments of Vink (unpublished) which showed that the EGL was restored in roughly 0.5 s after the passage of a white cell in a tightly fitting capillary. This model predicted EI to be ~700 pN nm^2, which is about 1/20 the measured value for an actin filament. This value of EI was more than sufficient to resist significant bending of the core proteins at physiological levels of FSS. Further experiments were then performed by Vink and a much more realistic large deformation "elastica" model developed to describe the restoration of layer thickness after the passage of a white cell as shown in Fig. 4a.[64] This refined model predicted that there were two phases in the fiber recoil; a fast phase I with large compressions and overlapping fiber tips parallel to the endothelial surface (<0.041 s), and a slow phase II where fibers assume a shape that is very similar to the solution for an elastic bar with linearly distributed loading (Fig. 4a). The predicted value for EI for this large deformation model was 490 pN nm^2. The electrochemical model of Damiano and Stace[30] attributes an electrochemical potential gradient and chemical gradient components in the EGL for its recovery after deformation. Figure 4b shows the comparison between the predictions of the elasto-hydrodynamic model (red line) to the predictions of the mechano-electrochemical model (triangles) and the experimental measurements (circles). The predictions of the electrochemical model have been questioned by Fu *et al.*[54] who predict a fixed charge density in the EGL which is ~30 times that of Damiano and Stace.[30] These models for the structural integrity of the EGL are central to understanding how FSS acting at the outer edge of the EGL is transduced

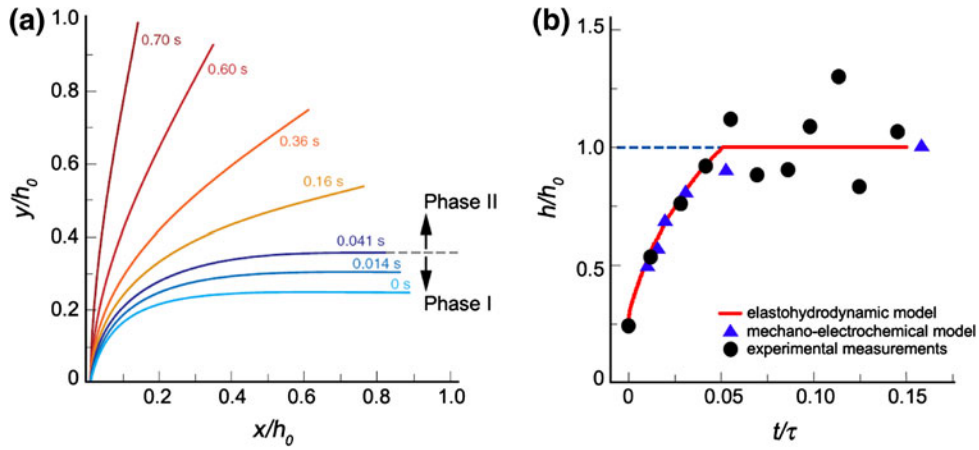

FIGURE 4. (a) The time-dependent change in shape of the core protein fibers in the EGL predicted by the elastohydrodynamic model. y/h_0 and x/h_0 are normalized vertical and horizontal axes of the fiber position with respect to the uncompressed thickness. Note the change from phase I to II occurs at 0.41 s. (b) Comparison of the elastohydrodynamic model (red line)[64] and mechano-electrochemical model predictions (blue triangles) obtained from Fig. 2b of Damiano and Stace[30] with the experiment measurements in Han *et al.*[64] The uncompressed EGL thickness = 400 nm. From Han *et al.*[64]

into the EC's actin cytoskeleton in the initiation of intracellular signaling in "Endothelial Cells" section.

Renal Epithelial Cells

The ultrastructural studies in "Renal Epithelial Cells" section strongly suggested that BBMV were an excellent candidate for mechanosensing. Previously it had been widely believed that the sole purpose of the BBMV was to greatly increase the absorption area. In 2000, Guo *et al.*[61] proposed that BBMV act as the mechanosensor and developed a theoretical model to predict the detailed velocity profile within the surface layer and the bending deformation of each microvillus. This model indicated that: (1) the velocity was greatly attenuated by the BBMV and nearly negligible except for the outer 5% of layer thickness; (2) the drag force is mainly concentrated at the tip of the MV and this force contributes ~85% of the total bending moment (torque) on the microvillus; (3) the deflection of the microvilli tips is so small (<4 nm for a microvillus of 2.5 μm length) that the BBMV act as stiff bristles that allow the transmission of torque to the ACW beneath the apical membrane; (4) although the predicted force on each microvillus is very small (<0.01 pN), Weinbaum *et al.*[174] showed using a moment balance that there is a nearly 40 fold amplification of the force arising from the resisting moment acting on the ACW at the base of the microvilli. This amplification is sufficient to deform the anchoring filaments in the actin cortical web and initiate signaling through linker molecules.[88]

The role of the primary cilium as a mechanosensor was first suggested by Schwartz *et al.*,[138] who noticed that the primary cilium in PtKt cells would undergo large bending deformations in response to fluid drag. An "elastica" model was proposed to determine the bending rigidity EI of the primary cilium and its change in shape with flow under the assumption that there is no rotation of the basal body inside the cell. They found that ciliary length appeared to be the key parameter in determining the bending moment at the base of the cilium and its sensitivity to the flow. The major limitation of this initial model was the assumption of constant fluid velocity and drag along the length of the cilium, which neglects both the FSS boundary layer and the interaction between cilia. The pioneering experiment of Praetorius and Spring[116] demonstrated that fluid flow not only triggers cilium bending, but elicits an increase of cytosolic Ca^{2+}. Removal of the primary cilia in MDCK cells abrogated this effect.[117] These experiments beautifully illustrated that this organelle has the capacity to be a sensory antenna to detect very small flow changes and initiate a physiological response, a calcium transient, which is important for the regulation of many different cellular processes. Liu *et al.*[93] proposed a more realistic fluid flow model, which considered both the interaction between cilia and its effect on the FSS velocity profile. The key findings for this model showed that the FSS in open flow chamber experiments in references[93] and[116] was only 1/10 that in the perfused tubule and that the fluid shear force on the apical surface of the cell was ten times larger than the drag acting on the cilia, although the latter produced the calcium signal. This result is consistent with a recent finite element model study by Rydholm *et al.*[133] which shows that the stresses in the membrane of the cilium are small except at its base. These authors also showed that the viscoelastic behavior of the membrane could account for the time-dependent of the calcium transient. A more recent mathematical model, which considers a FSS velocity profile and large bending deformations near the cilia base confirmed that the basal body of the primary cilium is firmly anchored allowing for a large resistance moment at its base.[68]

Dendritic Cells (Osteocytes)

As described previously, it had been widely believed that the sole function of fluid movement in the LCS was to provide nutrients and remove wastes. This view was radically changed in Weinbaum *et al.*,[172] who proposed that the fluid flow due to physiological loading proposed by Pikarski and Munroe[110] was the primary stimulus that enabled osteocytes to sense and respond to their mechanical environment. These investigators developed a mathematical model to predict the fluid flow induced FSS on the dendritic process membrane of the osteocyte due to physiological loading. The model predicted that flow induced physiological loading between 1 and 20 MPa generated FSS in the range of 0.8–3 Pa, which, quite surprisingly, is of the same level as FSS experienced by ECs in the vascular system. Several other computational models have since predicted the same level of FSS due to human and animal locomotion.[50,60,62]

Although the level of FSS predicted by these theoretical and computational models has been found to be sufficient to activate ECs, it is not clear whether this level of FSS on the osteocyte process membrane is sufficient to activate osteocytes, as the osteocyte process is much more rigid than the endothelial cell body owing to the existence of its densely packed central actin filament bundle.[183] Thus, a strain amplification model was proposed to investigate the contribution of lacunar-canalicular fluid flow from a different view point.[180] Instead of focusing on the FSS acting on the process membrane, You *et al.*[180] proposed that the stimulus was the drag force exerted by the fluid flow on

the pericellular matrix surrounding the cell processes. In this model the drag forces are transmitted by tethering filaments which attach the membrane of the cell process to the canalicular wall. The basic hypothesis was that the tension generated in the tethering filaments could lead to large cell membrane deformations in the hoop direction. These authors predicted that the very small whole tissue strains (<0.2%) could be greatly amplified (up to 100 fold) through the fluid flow interaction with the pericellular matrix, and the amplification increases with the frequency of the loading.

Two refined models were subsequently developed using the detailed ultrastructural observations summarized in "Dendritic Cells (Osteocytes)" section. Han *et al.*[63] considered the detailed fimbrin cross-linked hexagonal arrangement of the F-actin filament bundle and the measured spacing of the tethering filaments in You *et al.*[183] Han's refined model predicted that physiological loading of 20 MPa at 1 Hz could induce ~0.5% strain on the process membrane, which is just sufficient to trigger intracellular calcium responses *in vitro*.[184] The tethering filaments in Han's model were flexible, whereas there were also discrete more rigid attachments observed at periodic intervals along the canalicular wall where there were canalicular projections along the osteocyte process, as shown in Fig. 3c taken from McNamara *et al.*[104] Immunostaining suggested that that these local attachments were β_3 integrins. The theoretical model in Wang *et al.*,[170] which also included these more rigid attachments, predicted that the small whole tissue level strains could be amplified greatly in the axial direction in the vicinity of the integrin attachments sites (Fig. 5a). These axial strains, as large as 6% and more than 10 times the hoop strains predicted in Han's model, are sufficient to open stretched activated ion channels and initiate intracellular electrical-chemical signaling. Wang *et al.*[170] also predicted that forces on the integrin attachments due to the fluid flow in the LCS is 10 pN for a 20 MPa 1 Hz tissue level load, and 1 pN for a 0.1 MPa 20 Hz tissue level load (Fig. 5b). Since the apex of the conical projection is only 10–20 nm, there could be as few as a single integrin in the near contact region.

IN VIVO, *IN SITU* AND CELL CULTURE EXPERIMENTS TO VALIDATE THEORETICAL MODELS

Endothelial Cells

The roles of the EGL as a molecular sieve in determining the revised Starling force balance and as a barrier between blood cells and ECs in altering the hematocrit distribution in microvessels were discussed in "Endothelial Cells" section. In the present section we will focus our attention on the role of the EGL as a mechanotransducer of FSS in response to blood flow. It is well accepted that hemodynamic shearing forces acting on the endothelium play a central role in the regulation of vessel wall remodeling, transient and sustained cellular signaling, cytoskeletal restructuring, mass transport and atherogenesis.[31,153] ECs *in vivo* are constantly exposed to FSS that determine their shape and cytoskeletal organization. First indication that fluid flow had an influence on EC morphology was demonstrated *in vivo* by Flaherty and colleagues[48] who showed that after resecting an arterial patch at 90° to its original orientation, subsequent realignment was observed with the flow within 10 days. Evidence from numerous *in vivo* studies also indicated that ECs in the region where the shear stress is low (atherosclerotic regions) have polygonal morphologies with few stress fibers, while ECs in the high shear stress regions with unidirectional flow have elongated shapes with numerous stress fibers.[31] *In vitro* studies in

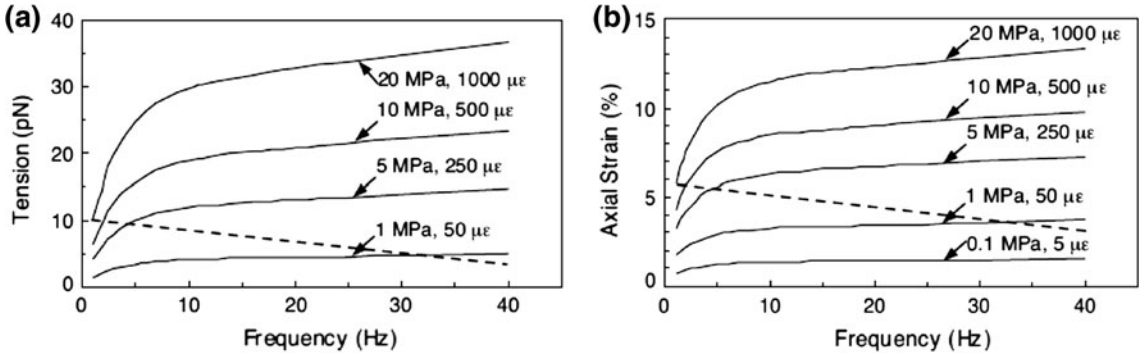

FIGURE 5. (a) The tension on the focal attachment T0 as a function of loading frequency with tissue-loading amplitude as a parameter. (b) The axial membrane strains ε_a in the vicinity of focal attachment complex as a function of loading frequency with tissue-loading amplitude as a parameter. From Wang *et al.*[170]

Galbraith *et al.*[55] showed three distinct EC adaption phases in response to 24 h FSS; phase I occurred within 3 h of FSS where cells began to elongate with more stress fibers and thicker intercellular junctions, phase II occurred after 6 h of FSS where there was a disruption of their dense peripheral actin bands (DPAB) and a shift of nuclei to the upstream region to the cell, and phase III began after 12 h of FSS where cells assumed elongated shapes in the direction of flow with thicker and longer stress fibers and increased substrate and intercellular adhesions. Recent studies by del Alamo *et al.*[32] observed similar EC remodeling in response to FSS using directional particle tracking microrheology.

Although it is clear that FSS plays a major role in EC mechanotransduction, the actual mechanics of the process of how EC senses and transmits the fluid shearing forces across the EGL was not well understood. The theoretical fluid flow models in "Endothelial Cells" section clearly indicated that fluid flow at the edge of the EGL was greatly attenuated by glycoproteins and proteoglycans in the EGL. Thus, the FSS acting on the apical membrane of the ECs was negligible.[29,47,139,140] This raised a fundamental paradox; how are mechanical and hydrodynamic forces transmitted across the EGL to the cell's intracellular cytoskeleton and, in particular, to the ACW beneath the apical membrane of the ECs and the DPAB, the structural support for the adherens junction. Key insights are suggested by the ultrastructural model sketched in Fig. 1f adopted from Squire *et al.*[144] and the elastohydrodynamic models in Weinbaum *et al.*[176] and Han *et al.*[64] These models predicted that the core proteins in the EGL are sufficiently stiff to transmit the fluid drag on their tips as a bending moment that acts on the ACW as shown in Figs. 6a and 6b and described in more detail in "Endothelial Cells" section.

Initial indication that the EGL serves as a mechanotransducer came from earlier *in situ* studies. Using rabbit arteries, Pohl *et al.*[114] and Hecker *et al.*[65] showed that when sialic acids or heparan sulfate proteoglycans were removed from the EGL by neuraminidase or heparinase, the flow-induced NO release was abolished whereas prostaglandin I_2 (PGI_2) was not. Subsequent *in vitro* experiments in Florian *et al.*[49] not only verified the presence of a heparan sulfate rich glycocalyx in cultured ECs, but also showed that the absence of glycocalyx by enzymatic digestion with Heparinase III abolished flow-induced NO production confirming the EGL's role as a mechanotransducer of FSS in NO release. A more comprehensive series of experiments was then undertaken by Thi *et al.*[159] to explore the role of the EGL under various conditions, presence [DMEM + 10% FBS, DMEM + 1% BSA], partial absence [Heparinase III + DMEM + 1% BSA] of heparan sulfate proteoglycans, and total

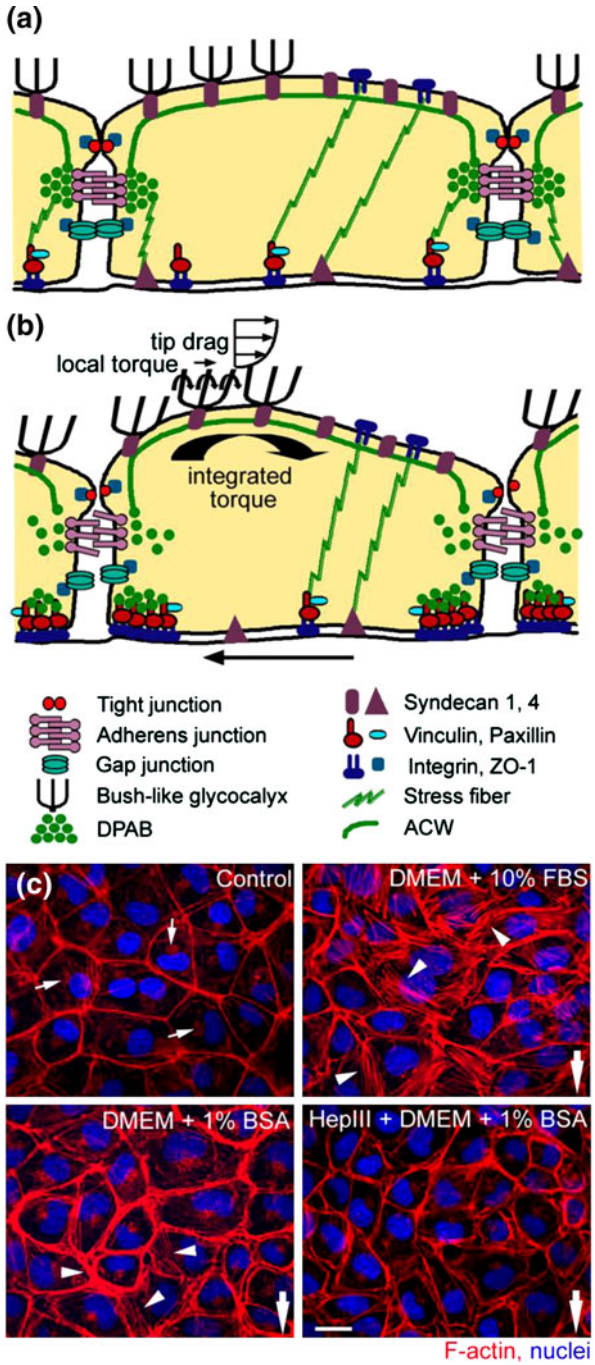

FIGURE 6. (a, b) Schematic representation of the conceptual "bumper car" model for the structural organization of the EC with intact EGL in response to FSS. (a) Under confluent control state, intact DPAB in ECs serves as a base for underlying actin cortical web (ACW) localized at the adherens junction just like a bumpers on a car. (b) Under fluid shear stress state, ECs respond to mechanotransduction across the EGL by reorganization of cytoskeleton and junctional and focal adhesion proteins. (c) Reorganization of EC cytoskeleton in response to fluid shear stress (FSS) of 10.5 dyne/cm^2 with various media: intact EGL media (DMEM + 10% FBS or DMEM + 1% BSA) and compromised EGL media (Heparinase III + DMEM + 1% BSA). F-actin (red) and nuclei (blue). Bar = 20 μm. From Thi *et al.*[159]

collapse of the EGL [DMEM alone] when cultured rat pad ECs were exposed to FSS of 10 dyn/cm^2 for 5 h. Changes in the cell cytoskeleton (F-actin), junction complexes (ZO-1, Cx43) and focal adhesions (vinculin, paxillin) were then examined for all three states of the EGL. The most noticeable findings from these experiments were observed under compromised EGL as shown in Fig. 6c; the typical augmented disruption of the DPAB and stress fiber formation in the presence of the EGL that had been frequently observed in previous studies was completely abolished when the EGL was compromised by the addition of Heparinase III or DMEM alone. Similarly, reorganization of vinculin and disruption of ZO-1 and Cx43 were observed only for an intact EGL. In marked contrast, the integrity of EGL had no affect on the distribution of paxillin, a marker for focal adhesion kinase (FAK) in the Src kinase pathway. These results unequivocally confirmed that the EGL served as a mechanotransducer of FSS.

The foregoing observations in Thi *et al.*[159] are explained using a conceptual "bumper car" model as shown in Figs. 6a and 6b. Under static conditions, the DPABs in the ECs acted as rubber bumpers on a car, which were held in lateral register with those of neighboring cells by the weak VE-cadherin linkages associated with the DPAB, which served as a peripheral base for the ACW under the apical membrane. When ECs were exposed to FSS, the integrated bending moments on the tips of the core proteins at the edge of the EGL caused a rotational moment on the ACW and DPAB that produced a clockwise rotation creating disjoining forces on the weak VE-cadherin linkages between cells as shown in Fig. 6b. The model predicted the disjoining force to be on the order of 70 pN in response to a FSS of 10 dyne/cm^2 which closely agreed with the 70–120 pN unbinding forces measured by Baumgartner *et al.*[13] Once these disjoining forces exceeded the weak adherens linkages, the unzipping of the adherens junction took place leading to a redistribution of F-actin, and the formation of stress fibers in the basal aspects of the cell. During the adaptation phase in response to FSS, there was migration of vinculin to cell borders to establish temporal focal adhesion at the edge of the cell until a new steady state was reached. When the EGL was compromised, the FSS acted directly on the apical membrane and the transmission of FSS was mostly from one EC membrane to the adjacent EC via the tight junction complex and stress fibers connecting the apical and basal surfaces to basal focal adhesion sites. This manner of transmission bypassed the underlying ACW and the DPAB complex allowing for direct transmission of FSS to basal integrin attachments. This conceptual model also explained why there was no change in the distribution of paxillin whether the EGL was intact or compromised, since the total traction force at the basal surface did not depend on the existence of EGL. Thus, the "bumper car" model provides two distinct endothelial cellular signaling pathways in response to FSS, one transmitted by the EGL core proteins as a rotational moment that acts on the ACW and DPAB and the other originating from focal adhesions and stress fibers connecting the basal and apical membranes as sketched in Davies.[31]

Subsequent studies performed by Yao *et al.*[179] confirmed the "bumper car" model predictions in Thi *et al.*[159] These experiments showed that when the EGL is compromised (Heparinase III treatment), ECs that typically realigned with the direction of flow failed to realign after exposure to FSS for 24 h as shown in Fig. 7 with no apparent changes in proliferation. In addition, the findings demonstrated that decreased migration rates and the formation of new adherens junction complexes observed for an intact EGL in response to FSS were largely absent in ECs with compromised EGL. The most striking finding from these 24 h experiments was the redistribution of heparan sulfate proteoglycans from a uniform surface expression to a distinct peripheral pattern relocating to the cell–cell junction region. This in turn suggested the EGL role as a mechanoadaptor which likely reduces the shear gradients that the cell surface experienced. Taken together, predictions and findings in Thi *et al.*[159] and Yao *et al.*[179] explained why ECs oriented in the direction of flow in the presence of FSS if they had an intact EGL. The elongation of ECs during FSS was to provide a longer base, thereby reducing the disjoining forces on the adherens junction and, thus, giving ECs greater stability when exposed to FSS. Aside being a mechanotransducer, the EGL also has been implicated in regulation of FSS-induced endothelial transport. A recent study by Lopez-Quintero *et al.*[94] showed that selective components of the EGL regulate NO-mediated hydraulic conductivity in response to FSS.

Renal Epithelial Cells

Experimental evidence for BBMV's mechanosensory role has been provided by several *in vitro* microperfusion studies of mouse PTs. Du *et al.* demonstrated that a fivefold increase in flow rate led to a twofold increase in both J_V and J_{HCO_3} (Figs. 8a and 8b).[38,39] At first glance, this would appear to contradict the classic *in vivo* experiment performed by Schnermann 40 years ago,[137] where the fractional Na absorption was constant when flow rate increased by a factor of 5. The theoretical model developed in Du *et al.*[38] shows that the torque on the microvilli is proportional to the flow rate Q, but inversely proportional to the square of the tubule diameter and that the latter increases

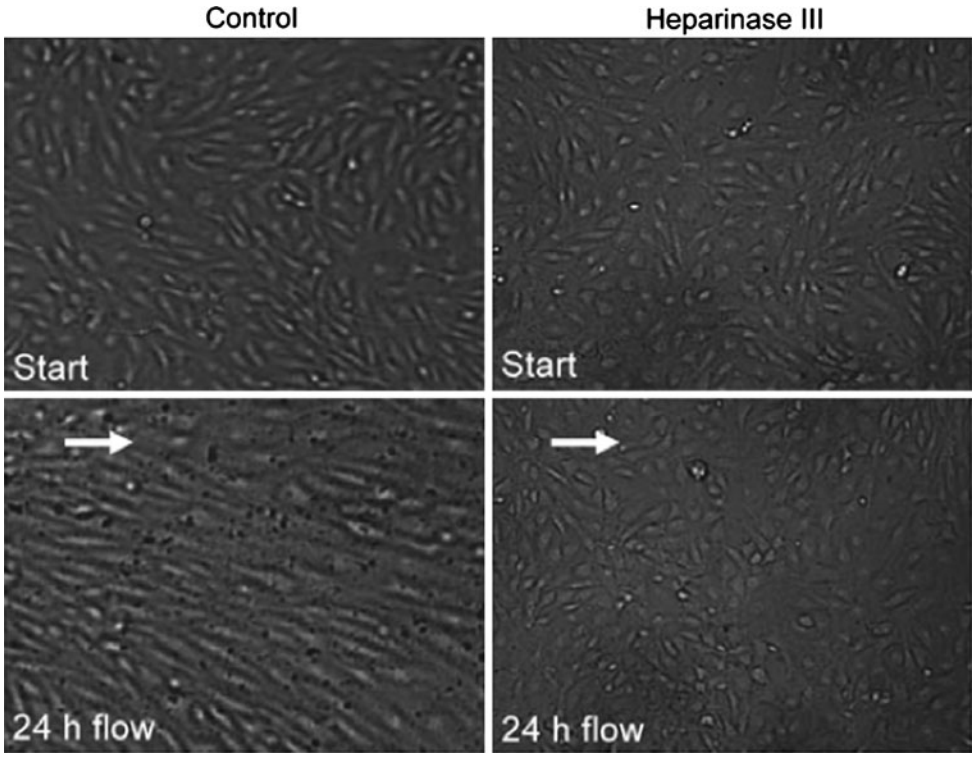

FIGURE 7. Evaluation of EC morphology after 24 h of fluid shear stress (15 dyne/cm^2) in the presence or the absence of EGL. While control EC monolayer aligns in the direction of the flow, EC monolayer with compromised EGL (Heparinase III treatment) fails to exhibit alignment. From Yao *et al.*[179]

significantly with the flow rate Q. In fact, a fivefold increase in Q is accompanied by a 50% increase of tubular diameter in the perfused mouse PT. When this increase in diameter was taken into account, it is found that both Na and HCO_3 reabsorption, J_V and J_{HCO_3}, scaled linearly with the bending moment on the microvilli (Fig. 8c) confirming the classic Schnermann observation. The significance of this study is two-fold. For the first time, a mechanical flow signal is directly linked to physiological responses, indicating that the hydrodynamic torque acts as an afferent signal to modulate PT Na and HCO_3 reabsorption in response to changes in luminal flow. Second, it explained a basic paradox, whether GTB exists *in vitro*. The classical counter example has been the Burg and Orloff[15] study on isolated rabbit tubules, in which the authors found that when flow increases three-fold, the J_v change was only 37%, far less than Schnermann's observation, a change that for four decades was thought to be insignificant. However, when taking into account the changes in tubule diameter in response to flow shown in Fig. 9a, one observes that the rabbit tubule is more compliant than the mouse (a 41% increase compared to 30% for the mouse). Applying the torque relation, one finds that there is a 38% increase in microvillus bending moment for the rabbit compared to a 61% increase for the mouse (Fig. 9b). If one now compares the bending moment and J_v, one observes a nearly perfect agreement between these two parameters (37% vs. 38% in rabbit, and 61% vs. 60% in mouse) (Fig. 9c). The linear change in J_v with GFR observed by Schnermann *in vivo* is mainly the result of PTs having only minimal circumferential stretch due to the small distensibility of the renal capsule wall.

According to the model predictions in "Renal Epithelial Cells" section, the two main components associated with the mechanosensing of fluid flow in CCDs are the bending moments on the primary cilium and the membrane strains at the cilium base. Three lines of evidence have been provided for the bending moment hypothesis. First, with a perfusion study done on split-open CCDs, Liu *et al.*[93] found that the flow-stimulated calcium (Ca^{2+}) response required a threshold flow rate of 3.2 μL/s. Increasing the flow from 3.2 to 25 μL/s resulted in a 2-fold increase in $[Ca^{2+}]_i$ (Fig. 10a).[93] A reduction of flow from 25 to 3.2 μL/s led to a fall in $[Ca^{2+}]_i$ back to baseline values measured at the initial slow flow rate. The magnitude of FSS at the fast flow rate is only 0.056 dyne/cm^2, a value well below the threshold for a Ca^{2+} response in ECs. Thus Liu *et al.*[93] suggested it is the torque acting on the basal body at the base of the cilium that triggers the calcium release.

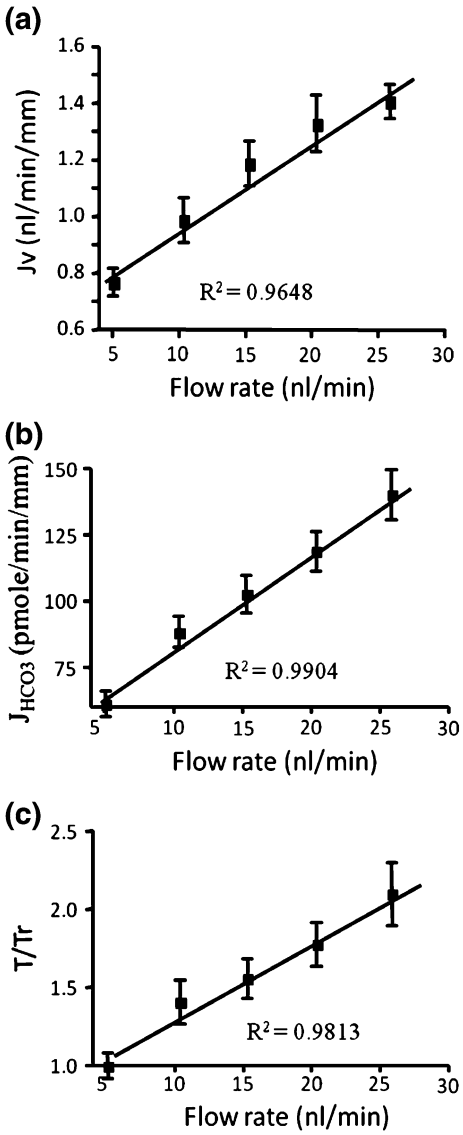

FIGURE 8. (a and b): torque-dependent Na and HCO_3 absorption. (c) torque ratio. Note that Jv and J_{HCO_3} scale linearly with T/Tr as flow rate increases. From Du *et al.*[39]

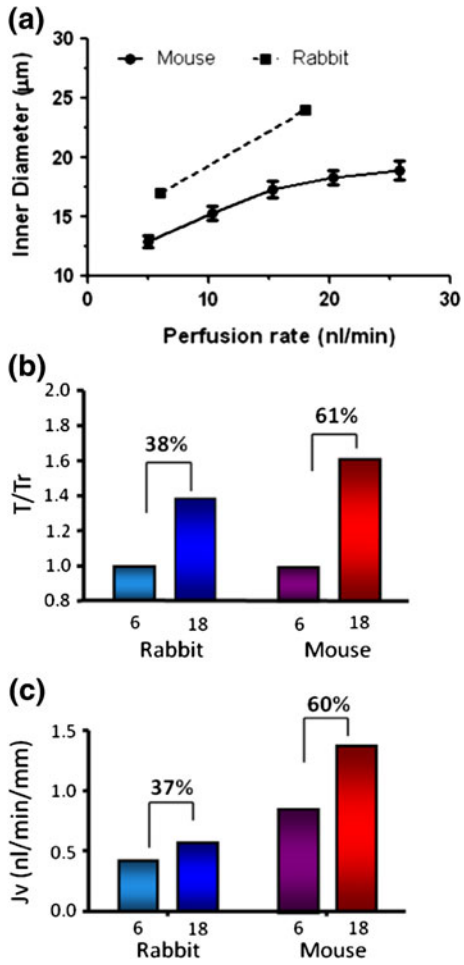

FIGURE 9. Flow-induced changes in PT transport. (a) inner diameter changes with increase in axial flow for mouse and rabbit. (b and c): torque ratio and reabsorption in mouse and rabbit PTs for 3-fold change in axial flow. From Du *et al.*[38] and Burg and Orloff.[15]

Second, shortening or removal of cilium blunts the flow-dependent cellular responses. In *orpk* mice, cells with stunted cilia within dilated portions of cystic CCDs had a minimum increase of $[Ca^{2+}]_i$. Similarly, shortening of the cilium length of cultured cells by orbital shaking or treatment with chloral hydrate led to a decreased or non-responsive transepithelial ENaC current.[129] Third, Using laser tweezers, Resnick *et al.*[128] applied mechanical forces directly to the apical surface of MDCK cells and found a null intracellular Ca^{2+} response indicating that the apical membrane does not participate in mechanotransduction. Collectively, these results strongly suggest that primary cilia are the mechanosensing organelle in the CCD.

The bending of the ciliary axoneme is unlikely the sole reason for the flow-activated Ca^{2+} response, since the tip deflection for a 2.5 μm cilium at even the higher flow rate of 25 μL/s was theoretically predicted to be <2 nm.[93] Rydholm *et al.* further showed that the stresses in the membrane of the cilium are small, except at the base.[133] In fact, only the forces at the base of the cilium are large enough to produce physiologically significant strains. Recently, a large body of molecular evidence has emerged from the studies of the dysfunction of renal epithelial cells in polycystic kidney disease (PKD), which depict the base of the cilium as a hot spot for mechanotransduction. For example, the activation of transmembrane proteins polycystin 1 and 2, localized to the ciliary base, has been suggested to be mediated by flow and the subsequent release of Ca^{2+} from intracellular stores. Centriole orientation is also

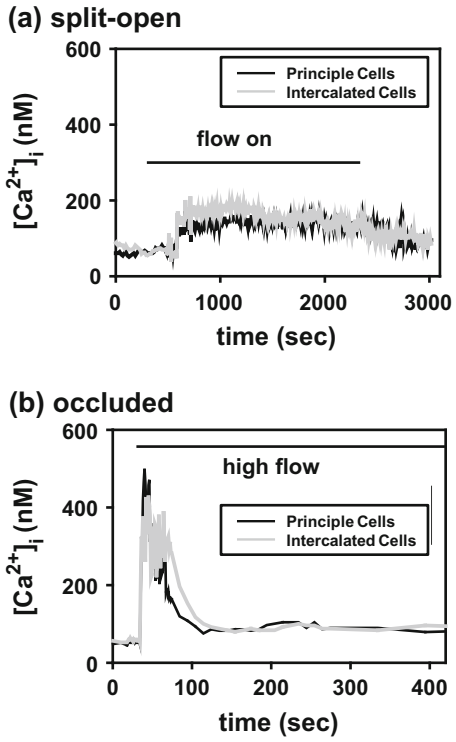

FIGURE 10. Representative traces of intracellular Ca^{2+} concentration responses of principal and intercalated cells to acute increase in superfusate flow rate in a split-open CCD (a), and circumferential stretch in an occluded CCD (b). Horizontal bars indentify onset and termination of high flow. From Liu *et al.*[93]

modulated by ciliary flow sensing.[82] It is not clear how polycystin 1 is activated on the molecular level. A possible explanation might be that the torque induced strains acting at the cilium base lead to polypeptide unfolding and release of domain-domain interactions which activate the ciliary-targeted proteins.

To determine whether circumferential stretch is also involved in mediating the flow-induced Ca transient, an occluded CCD model was used in Liu *et al.*[93] In occluded CCDs, a rapid increase in luminal volume, sufficient to increase tubular diameter by only 5%, led to a twofold increase in $[Ca^{2+}]_i$, whereas a slow expansion of tubular diameter by 20% failed to elicit a Ca transient. These observations suggest that the trigger for the flow-induced Ca^{2+} response is not likely circumferential stretch, but rather the magnitude of the FSS and the resulting torque on the cilium. In occluded CCDs, peak Ca^{2+} was reached within 10 s compared to ~30 s in the split-open CCDs after onset of the flow (Fig. 10b). The discrepancy was explained by the difference in cellular viscoelastic properties between the split-open CCDs and intact CCDs. This is explained in more detail in the finite element study by Rydholm *et al.*[133]

At the molecular level, Weinbaum *et al.*[174] has proposed that the actin cytoskeleton, the main component of BBMV, is the key mediator that transmits the afferent hydrodynamic signal into intracellular signaling. In mouse PTs, the addition of the actin disrupting drug (cytochalasin D) eliminated the flow-dependent increase in J_V and J_{HCO_3}.[38,39] To explore this further cell culture studies were conducted to investigate the cytoskeletal reorganization at the molecular level due to flow stimulation.[40] When cultured under static conditions, mouse PT (MPT) cells demonstrated numerous pronounced cytosolic actin stress fibers on their basal membrane. FSS induced the disappearance of stress fibers from the basal surface and a reinforcement of the lateral actin network.[40,43] A FSS of only 1 dyne/cm^2 led to a formation of tight (TJs) and adherens junctions (AJs), and an accumulation of focal adhesion proteins (vinculin and paxillin) in the basement membrane.[40] These findings are surprisingly opposite to that observed for confluent EC monolayers.[159] In addition, ECs require a 10-fold higher FSS to induce cytoskeletal changes. This discrepancy between the ECs and PTCs in response to FSS was explained by a "junction buttressing" model for the PT cells.[40] In static control cells, strong expression of stress fibers on the cell base causes a firm attachment of the cells to their substrate. This creates a tension on the cell lateral membrane accompanied by a compressive resistance of the internal cytoskeleton, which results in a rounded canopy at the apical membrane and the pulling away of the cell from its neighbors. Cell junctions cannot form until there is a disruption of the stress fibers at the basal surface and a release of this membrane tension. A small FSS applied to the apical surface was able to create a large enough rotational moment at the cell base to cause these tall cuboidal cells to tilt, and their basolateral surfaces to come into contact. This leads to the formation of TJs, AJs and a DPAB. In comparison, Thi *et al.*[159] have proposed for ECs that the DPAB with its vascular endothelial-cadherin bonds function like a "rubber bumper" in the static control condition. Unless the rotational moment applied on the endothelial glycocalyx at the apical surface of the ECs exceeds the resisting moment provided by the DPAB with its AJ, cytoskeletal reorganization will not take place. The large difference in effective lever arm provided by the tall cuboidal epithelial cells compared to the flat ECs is the main reason that a FSS of only 1/10 that applied in the ECs is necessary for epithelial cells to undergo cytoskeletal reorganization.

Similarly, flow-induced increase of intracellular calcium in murine embryonic kidney (MEK) cells has been found to be closely dependent on a dedicated global cytoskeletal control.[5] Disrupting cytoplasmic

microfilaments or microtubules in these cells eliminated calcium response. Altering the cytoskeletal force balance by inhibiting actomyosin-based tension generation (using 2,3-butanedione monoxime), interfering with microtubule polymerization (using nocodazole, cochicine, or taxol), or disrupting basal integrin-dependent extracellular matrix adhesions (using soluble GRGDSP peptide or anti-h1 integrin antibody), also inhibited the calcium spike in response to FSS.

Dendritic Cells (Osteocytes)

In "Dendritic Cells (Osteocytes)" section we have described various fluid flow models for the LCS in bone. In this section we describe cumulative experimental evidence supporting the fluid flow hypothesis for mechanotransduction in the LCS when bone is subjected to mechanical loading. There are two categories of experimental studies that explore interstitial fluid flow through the pericellular matrix of the LCS in bone, tracer studies and FRAP studies.

Tracer Studies

In these experiments, tracers of various sizes were injected into the vascular system of animals and the tracer distribution in bone matrix were examined and quantified at different time points after the tracer injection.

Tracer studies were first conducted in the absence of applied external loading to track fluid movement in bone. Using a large tracer molecule ferritin (~12 nm in diameter), Dillaman,[33] Montgomery *et al.*,[106] and Qin *et al.*[124] found that shortly after injection ferritin staining was found mainly confined to the vascular canals and showed halo-shaped labeling around the osteonal canal (the canal in cortical bone containing blood vessels). More recently, Wang *et al.*[166] and Ciani *et al.*[26] (Fig. 11b) demonstrated that the halos were likely an artifact of histological processing, suggesting that this 12 nm large tracer cannot penetrate the pericellular matrix of the LCS.

Conversely, most studies using a medium-sized tracer, horseradish peroxidase (~6 nm in diameter)[37,81,166] and small-sized tracers, microperoxidase (~2 nm diameter) and procion red (~1 nm diameter)[8,81,152,166] have shown that these tracers are confined to the LCS, but missing from the mineralized matrix (Fig. 11a), indicating that molecules ≤6 nm can penetrate the pericellular matrix surrounding the osteocyte processes. Collectively, these results validate theoretical model predictions in that: (a) there is transport in the LCS; (b) the size of pores of the pericellular matrix in the LCS falls in the range of 6 nm to 12 nm, which is consistent with the predicted mesh size, 7 nm, of the pericellular matrix first proposed by Weinbaum and colleagues[172]; and (c) there is little or no transport at the level of the collagen-apatite porosity.

More recently, investigators have used tracer methods to test whether external loading will enhance the transport in the LCS due to fluid flow. Both *in situ*[79] and *in vivo*[80,97,148] loaded animal tracer experimental studies demonstrated higher concentration of tracer, higher number of periosteocytic spaces exhibiting tracer, and increased penetration of tracers in the pericellular space surrounding osteocytes in loaded as compared to non-loaded bone, indicating that external applied mechanical loading dramatically enhances fluid flow in the LCS. This enhancement in transport could not occur if water could leak through mineralized boundaries of the LCS.

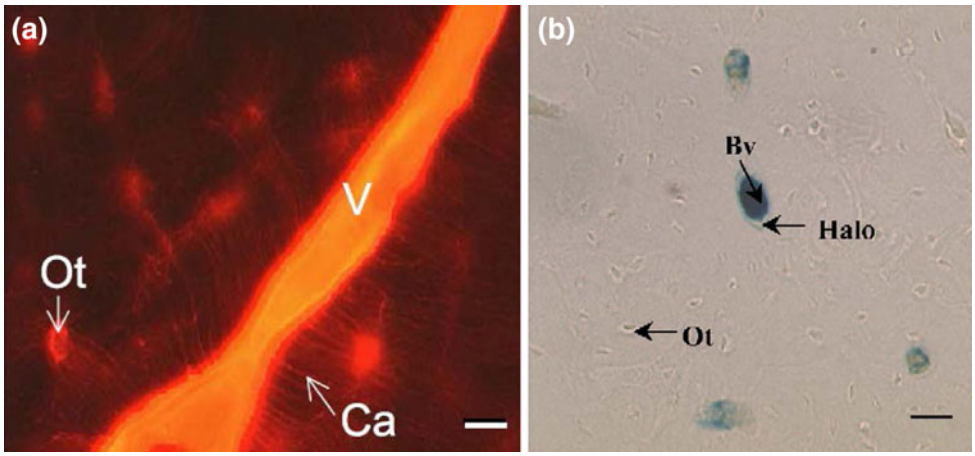

FIGURE 11. Left: Tracer labeling at the posterior medial region of the rat tibia. Reactive red appeared in most blood vessels (v) and osteocytic lacunae (Ot) (magnification: 350×, scale bar: 40 mm). From Wang *et al.*[166] Right: Ferritin distribution for the different histological processes. Ferritin was primarily confined to the bone blood vessels (Bv) with the sporadic presence of ferritin "halos" surrounding blood vessels (magnification: 900×, scale bar: 15 mm). From Ciani *et al.*[26]

FRAP Studies

Wang *et al.*[169] developed a novel technique which combines fluorescence after photobleaching (FRAP) with confocal microscopy to directly measure real-time solute movement in intact bones. In this study, the movement of a vitally injected fluorescent dye between individual osteocytic lacunae was visualized *in situ* with laser scanning confocal microscopy. Transport was analyzed and the diffusion coefficient of fluorescein was determined to be ~3.3×10^{-6} cm^2/s, which is consistent with the presence of an osteocyte pericellular matrix with mesh pore size being ~7 nm as predicted in the theoretical model of Weinbaum and colleagues.[172]

Su *et al.*[147] extended this approach by investigating the effect of externally applied loading on the fluid flow in bone in a mouse femur *in situ*. These researchers found that the applied loads significantly shortened the fluorescent intensity recover time by 24% compare to non-loading controls, indicating the fluid flow in cortical bone is enhanced by externally applied mechanical loading.

In the latest study, Price *et al.*[120] performed FRAP measurements on loaded bone *in vivo*. They demonstrated that cyclic and physiological level compression of the mouse tibia significantly enhanced (+31%) the transport of sodium fluorescein through the LCS when compared to diffusion alone (Fig. 12). By combining FRAP and computational modeling, the peak canalicular fluid velocity in the loaded bone was predicted (60 μm/s) and the resultant peak FSS at the osteocyte process membrane was estimated (~5 Pa). This study convincingly demonstrated the presence of load-induced convection in mechanically loaded bone. Using a similar approach, Kwon and coworkers[85,86] combined FRAP and computational modeling to estimate the peak interstitial fluid flow velocity in hindlimb suspended mice due to enhanced intramedullary pressure. Their findings suggest that the increase in intramedullary pressure increases interstitial fluid flow in bone and leads to a peak fluid flow velocity of 130 μm/s in the LCS double that of Price *et al.*[120] where the fluid flow in the LCS is driven by externally applied mechanical load. It is very difficult to reconcile these two predictions since the increased intramedullary pressure in the LCS in the hind limb model is two orders of magnitude lower than the interstitial fluid pressures generated by mechanical loading on bone.[167] Therefore, it is not clear how these two very different loading models have led to similar levels of flow velocity in the LCS. This paradoxical prediction is of special interest since oscillations in intramedullary pressure have been demonstrated to produce new bone formation and inhibit bone loss at the endosteal surface.[123] Collectively, these *in vivo* FRAP loading experiments have, for the first time, provided direct unequivocal observation and quantification of load-induced fluid and solute convection through the LCS.

Cell Culture Experiments

Since fluid flow has been proposed as the most likely mechanical candidate for activating osteocytes, many *in vitro* studies have been performed examining various aspects of fluid flow on osteocytes. These studies show that osteocytes are very sensitive to fluid flow and elicit a wide range of biochemical responses. We summarize below the recent progress in *in vitro* experimental studies on osteocyte mechanosensitivity to various fluid flow protocols at the theoretically predicted level of FSS generated under physiological loading (0.8–3 Pa).[172]

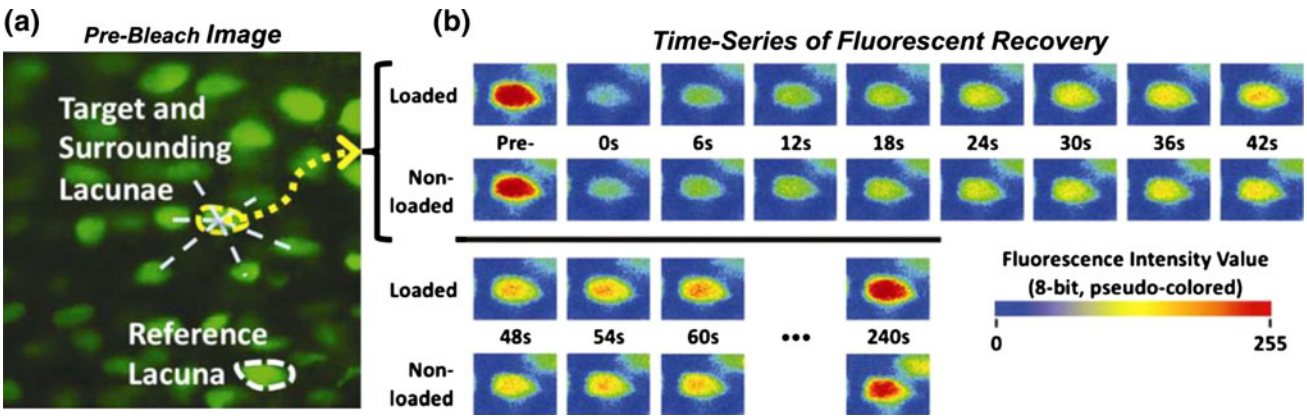

FIGURE 12. A representative pair of FRAP experiments with sodium fluorescein (376 Da) in a murinetibia subjected to cyclically loaded (peak load of 3 N at 0.5 Hz with a 4 s resting/imaging period between two cycles) or non-loaded paired tests. (a) Pre-bleach image showing a cluster of osteocyte lacunae chosen for FRAP imaging, including the target (outlined in yellow) and surrounding lacunae, along with a reference lacuna (outlined in white) for autofading correction. (b) The time-courses of fluorescence recovery within the same photobleached lacuna under loaded or non-loaded conditions. From Price *et al.*[120]

Osteocytes have been shown to be able to respond to pulsating fluid flow (PFF) with increased release of prostaglandin E_2 (PGE_2), increased nitric oxide (NO) synthesis,[77,78] inhibited osteocyte apoptosis,[149,151] increased intracellular calcium mobilization,[9] and upregulated gene expression of proteins involved in Wnt signaling pathways.[135] Furthermore, the conditioned medium from these PFF stimulated osteocytes were shown to inhibit proliferation, but stimulate differentiation of osteoblasts,[162] and inhibit osteoclast formation and bone resorption.[150]

Application of steady fluid flow (SFF) on osteocytes leads to opening of gap junctions, redistribution of Cx43 protein and delayed effects on Cx43 protein expression,[21,22] increased PGE_2 release,[18] and inhibition of osteocyte apoptosis.[76] Oscillating fluid flow (OFF) applied on cultured osteocytes has been shown to establish more gap junctions,[6] increase intracellular calcium mobilization (in terms of both percentage of cells responding and the magnitude of response), increase PGE_2 release,[98,127] activate gap junction and adenosine triphosphate (ATP) release,[57] and inhibit osteocyte apoptosis.[24] The conditioned medium from OFF stimulated osteocytes inhibits osteoclastogenesis through regulation of receptor activator of nuclear factor kappa B (NF-κB) ligand (RANKL) and osteoprotegerin (OPG) expression.[181]

While many studies have been performed on the effect of different flow protocols on osteocytes, there are relatively few studies which have investigated how the responses of these different protocols differ. By comparing OFF and SFF, Ponik *et al.*[115] observed that these two different types of fluid flow stimuli can induce significantly different responses from osteocytes in terms of regulation of cell morphology, cytoskeletal organization, and gene level expression of osteopontin.

Most *in vitro* osteocyte fluid flow studies are conducted using conventional parallel plate flow chambers, where the responses from osteocyte processes and osteocyte bodies cannot be differentiated. Recently, several new approaches have been developed to address this concern. You *et al.*[182] developed a prototype microchannel system that attempts to qualitatively simulate the LCS *in vivo*. Such a system will help to identify the cellular pathways in osteocyte mechanotransduction. Targeted to differentiate the mechanosensitivity of the osteocyte process and cell body, Adachi *et al.*[1] used a glass microneedle to apply separate local deformations on the osteocyte process and cell body. They observed a significantly larger calcium response in cell processes than in cell bodies, and a larger deformation was necessary at the cell body to induce a calcium response and concluded that mechanosensitivity of the processes was higher than that of the cell body. Moreover, recent findings in Burra *et al.*,[19] where they managed to differentially stimulate osteocyte cell processes and body using a transwell system, show that integrin attachments along osteocyte cell processes act as mechanotransducers. Subsequent studies by Litzenberger *et al.*[92] demonstrated that PGE_2 release is mediated by β_1 integrin. Most recently, Wu *et al.*[178] developed a novel Stokesian fluid stimulus probe to focally apply pico-newton level hydrodynamic forces of the magnitude predicted in Fig. 5b along the processes[170] and on the cell body using micropipette injection at extremely low tip Reynolds numbers. Most strikingly, large increases in electrical conductance were observed only when the pipette tip was directed at local integrin attachment sites along the process, but not on the cell body or on portions of the process that were not attached to the substrate. This new approach clearly demonstrated that forces between 1 and 10 pN could open stretch activated ion channels along the processes at points of integrin attachment, initiating electrical signaling that could be easily detected by whole cell patch clamp measurements.

Another potential osteocyte mechanosensing mechanism proposed by Jacobs and coworkers[7,75,87,98,156] has recently received considerable attention. These investigators observed that single primary cilia extended from the cell body into the extracellular space both *in vitro* and *in vivo*. OFF *in vitro* induced osteocyte responses (e.g. RANKL/OPG ratio, PGE_2 release, cyclic adenosine monophosphate (cAMP) release) which were eliminated with cilia removal, suggesting that primary cilia act as mechanosensors of fluid flow. How the long primary cilia (~2–9 μm) observed *in vitro* could either fit or function in the narrow pericellular space between osteocyte body and the lacunae wall (~1 μm) leads one to question what function they perform *in vivo*. A key observation is that fluid flow does not seem to elicit a calcium response in bone cells *in vitro* in marked contrast to renal cells in the CCD where the primary cilia are free to deform under FSS. The latest study by McNamara *et al.*[103] in mice tibia shows that cilia are present only in lacuna in close proximity (25 μm) to the periosteal surface, that these cilia are parallel and not perpendicular to the cell body surface and, thus, could not bend in response to fluid flow under these confined conditions. McNamara *et al.*[103] propose that bone cell cilia are only present in newly generated bone, that they are chemical rather than fluid flow sensors, and that their function may be associated with mineralization processes at the bone cell surface when the pericellular space is first formed. Future studies need to be carried out to further elucidate the role of primary cilia in bone and why they disappear in mature bone.

DOWNSTREAM SIGNALING

Endothelial Cells

Numerous studies indicate that ECs respond to FSS by activating a variety of signaling pathways that typically lead to modulation of gene/protein expression (Rho, focal adhesion kinase [FAK], Src, integrins, Krupple-like factor-2 [KLF-2]), release of signaling molecules (prostaglandins I_2 [PGI_2]), nitric oxide [NO], Ca^{2+}) and ultimately regulation of cellular function. These downstream signaling pathways most likely contribute in regulating endothelial functions that are needed during vascular development and remodeling. Primary evidence that FSS-induced directional EC migration through the Rho signaling pathway during wound healing came from studies in which inhibition of Rho with C3 exoenzyme reduced EC migration under flow.[70] Since Rho activity is linked to activation of either FAK or Src, subsequent studies used a green fluorescence protein (GFP)-tagged FAK to investigate the molecular dynamics of FAK at focal adhesion sites in migrating ECs in response to FSS.[89] They showed that besides colocalizing with phosphorylated FAK (Y397), GFP-FAK was recruited to new focal adhesion sites to support the protrusion of lamellipodia at the leading edge after FSS. Given that tyrosine phosphorylation of FAK allows FAK to interact with Src, which is a known regulator of integrin-cytoskeletal interaction,[142] Wang *et al.*[165] was able to show the transmission of mechanically induced Src activation in live cells using a fluorescent resonance energy transfer (FRET) based Src indicator. They demonstrated that the mechanically stimulated Src activation was a dynamic process that guides local activated signals to spatial destinations throughout the cytoskeleton. More recently, Goldfinger *et al.*[59] showed that shear-induced α4 integrin phosphorylation was associated with cytoskeletal alignment in ECs. They found that endothelial α4 integrin became phosphorylated under a physiological FSS and that this phosphorylation was blocked by inhibitors of cAMP-dependent protein kinase A (PKA). Since PKA is known to be involved in the alignment of shear-induced ECs, they further suggested that phosphorylated α4 integrin is involved in establishing the directionality of ECs in response to FSS. Moreover, experiments in Wang *et al.*[25,168] indicated that continuous expression of Krupple-like factor-2 (KLF-2) during FSS is crucial to EC survival. Inhibition of KLF-2 with siRNA reduced EC viability in response to oxidized LDL-induced apoptosis, indicating a protective role of KLF-2 during FSS-induced apoptosis.

ECs respond to FSS by releasing well known vasoregulators such as NO and PGI_2.[65,114] As demonstrated by Kuchan *et al.*[84] NO release in response to FSS exhibits a biphasic behavior; a rapid and transient production phase (2–5 min) that depends on Ca^{2+}-Calmodulin and G-protein pathways and a sustained production phase that depends on FSS.[83] The release mechanisms of FSS-induced NO have been linked to specific increases of eNOS.[49,160] Similarly, FSS-induced PGI_2 release in ECs has two phases: an initial burst and steady state production that relies on an exogenous source of arachidonic acid and is directly regulated by the magnitude of the FSS.[51,65] More recent studies have revealed that shear-induced NO release was also regulated by the EGL.[49,112] Using selective enzymes to remove the specific components of the EGL these studies illustrated that removal of chondroitin sulfate had no effect, while removal of heparan sulfate and sialic acid blocked the FSS-induced NO release. In addition, none of the three enzymes used had an inhibitory effect on FSS-induced PGI_2 production, thus demonstrating multiple mechanisms for shear-induced release of signaling molecules.[112]

Renal Epithelial Cells

Na and HCO_3 transport in PT mainly depends on the activity of membrane transporters on both the apical and basolateral domains.[96,119] Knowing that flow regulates Na and HCO_3 reabsorption, we next want to explore flow stimutated membrane transporter activity. As a prelude to these experiments Weinstein *et al.*[177] have developed a theoretical model examining the coupling of transporters at the apical and basolateral membranes employing the torque dependent hypothesis in references.[38,39] The model shows that this linkage is essential for cell volume homeostasis. Using an immortalized cell line (mouse PT cells), Duan *et al.* performed Western and confocal analyses on the localization and expression of the membrane transporters (NHE3, V-ATPase, and Na/K-ATPase) under static and flow conditions.[41] They found that FSS induces NHE3 and V-ATPase synthesis, and luminal protein trafficking to the apical plasma membrane. When adding cytochalasin D into the perfusate, the flow-dependent NHE3 was completely abolished, whereas V-ATPase was not affected at all, showing consistent staining pattern with the static condition. On the other hand, colchicine inhibited the V-ATPase activation in response to flow. This indicates that mechanotransduction in PT cells is not limited to the actin cytoskeleton, but the entire cytoskeletal network including the microtubule cytoskeleton. On the basolateral side, FSS stimulated the upregulation of the total cellular pool of Na/K-ATPase and a translocation to its active membrane domain. This study

provided strong evidence for the validity of the Weinstein *et al.* model, in which the importance of a coordinated scaling between luminal and peritubular transport activity had been emphasized.[177]

So far the detailed downstream signaling of flow in PTs still remains unclear. Several scenarios have been proposed: (1) The mechanotransduction cascade begins with the torque on the microvilli which activates the mechanosensitive linker proteins located on the microvilli and then results in the activation of membrane transporters that directly or indirectly interact with them. For example, ezrin, connecting with NHE3 via specific proteins, has been shown to have regulatory effect on NHE3 translocation and activation.[188] Further studies on mutant mice with defective microvilli (ezrin KO mice) would be of great interest. (2) Secondary messengers, such as calcium, angiotensin II (AngII), and nitric oxide, are important regulators of PT Na^+ and HCO_3^- transport.[101] FSS induces AT1 receptor externalization from condensed apical recycling endosomes in cultured mouse PT cells, indicating that fluid flow is important for directing AT1 receptors to the apical surface and allowing them to interact with AngII to produce cellular signals. Whether AngII plays a role in flow-activated PT transport has not been reported.

In the distal nephron and CCD, flow-induced bending of the cilium apparently results in conformational changes of polycystin-1 that transduce the mechanical signal into a chemical response via activation of associated polycystin-2, which functions as a calcium channel.[108] Once calcium crosses the plasma membrane via this mechanically triggered pathway, it induces release of additional calcium from intracellular stores via a ryanodine-sensitive mechanism that further amplifies the subsequent cellular response.[108] Fluctuations in luminal flow could also generate regular oscillations in intracellular calcium, which could serve to regulate activity of ion channels. For example, slow calcium oscillations (3–5 min between peaks) have been shown to activate the transcription factor NF-κB, which in the developing kidney leads to increased cell proliferation and protection from apoptosis. These signaling pathways have been suggested to contribute to flow-induced Na reabsorption and K^+ secretion and increase the lumen-negative transepithelial potential differences.[136]

Dendritic Cells (Osteocytes)

Many *in vitro* studies have shown that osteocytes are capable of responding to fluid flow with various biochemical responses both intracellularly and/or intercellularly between both neighboring and effector cells by transiently increasing intracellular calcium $[Ca^{2+}]_i$ levels, altering expression of gap junction protein Cx43, and releasing mechanosignaling molecules (ATP, PGE_2, NO, and vascular endothelial growth factors [VEGF]). In this subsection we briefly summarize these biochemical responses due to FSS in a variety of cell culture experiments.

It has been shown that this cell–cell communication is critical for bone metabolism and function, and it is regulated by fluid flow.[36] Similar to ECs and osteoblasts, osteocytes respond to FSS with an increase in intracellular Ca^{2+} concentration,[127] which has been shown to regulate gap junction communication. First indication that FSS regulated Cx43 expression in osteocytes was reported by Cheng *et al.*[22] who showed that junctional communication increased after 30 min exposure to FSS; this temporary increment decreased after 24 h post FSS. Subsequent experiments in Thi *et al.*[157] showed disrupted junctional expressions of Cx43, Cx45, and ZO-1 in response to different magnitudes of FSS at 1 to 3 h exposure times. Since turnover rate of Cx43 is between 1 and 3 h, the inconsistencies between the results of Cheng *et al.*[22] and Thi *et al.*[157] could be due to differences in exposure time.

It is well established that PGE_2, ATP and NO are important cell–cell signaling molecules that are associated with bone's anabolic response to mechanical loading. Key evidence that FSS induced PEG_2 release in osteocytes was first reported in Klein-Nulend *et al.*,[77] where a significant release of PGE_2 was seen after only 10 min of FSS. Reilly *et al.*[127] subsequently demonstrated that the glycocalyx or pericellular matrix in osteocytes played an important role in mechanotransduction; they showed that removing the glycocalyx using hyaluronidase significantly reduced FSS-induced PGE_2 release without affecting the FSS-induced intracellular Ca^{2+} signal. Findings from this study suggest that FSS-induced PGE_2 release is most likely associated with integrin attachment sites on osteocytic cell processes which are released after hyaluronidase treatment. Recent findings in Cherian *et al.* further demonstrated using gap junction blockers that the release of FSS-induced PGE_2 was through Cx43 hemichannels (half gap junctions) in osteocytes.[23] On the other hand, accumulating evidence suggests that extracellular ATP and its cell surface receptors (purinoceptors; P2Rs) also play crucial roles in bone mechanotransduction. Using a $P2X_7R$ null mouse model and $P2X_7R$ specific blockers, Li *et al.* demonstrated in cell culture that the FSS-induced ATP signaling pathway is through $P2X_7R$ pore formation and subsequent PGE_2 release.[91] In contrast, studies in Genetos *et al.* indicated that FSS-induced ATP release from osteocytes occurred through Cx43 hemichannels.[57] These differences in findings of which channels assist the release of mechanosignaling molecules have yet to be resolved.

Osteocytes also respond to FSS by rapidly releasing NO within 5 min after flow initiation.[77] NO has been shown to mediate not only the inhibition of osteocyte apoptosis by FSS[149] but also the activation of the canonical Wnt signaling pathway.[134,135] Moreover, osteocytes have also been shown to release other mechanosignaling molecules such as soluble RANKL (sRANKL), OPG,[181] and VEGF.[24,158] Through the regulation of these soluble factors, fluid flow can indirectly regulate the function of other cell populations such as, osteoblasts, osteoclasts and endothelial cells, which in the end leads to the regulation of the bone remodeling process.

SUMMARY COMPARISON

In Table 1 a brief summary is presented comparing key aspects of the ultrastructure and flow dependent mechanisms in ECs, renal epithelium in the PT and CCD and osteocytes.

From an ultrastructural and mechanosensing viewpoint Table 1 reveals that the three basic cell types adapt to their mechanical environment in quite different ways, since the FSS varies greatly from ≤0.05 Pa to 3 Pa and the basic cell geometries are so different. ECs and osteocytes are surrounded by a pericellular matrix of glycoprotein's and proteoglycans that are superficially similar in that both transmit fluid forces to an intracellular actin cytoskeleton. However, in the case of ECs the signaling is an integrated response due to FSS acting over the entire apical membrane of the cell, whereas for osteocytes this signaling appears to be initiated at discreet focal attachment sites, which are independent of Ca^{2+} release, and involve a mechanically sensitive ion channel permeable to molecules such as ATP and PGE_2. This sensing, which is much more sensitive (in the pN as opposed to the nano-N force range), can be only detected by whole-cell voltage-clamp techniques. PT cells appear to be similar to ECs in that the mechanosensing structure covers the entire apical surface and serves as a sensor of FSS. The FSS produces an integrated moment on both cell types which act at the level of the adherens junctions. The primary difference is that in PT cells the torque on the cell leads to the insertion of transporters which are needed for water (Na^+) and H^+ transport. There is no significant active transport in ECs. Primary cilia in the CCD are a distinctly different structure which appears to play a crucial role in Ca^{2+} signaling where FSS is extremely small. Though primary cilia also present initially on the cell body of osteocytes, they are not likely flow sensors, but may serve as a chemical sensor of the pericellular space surrounding the cell body in its lacuna. Bone cells differ from the other two cell types in that the mechanical strains in their *in vivo* environment are so small that they need to be greatly amplified at the cellular level to be detected. As already noted that they need to be responsive to pN level forces.

One of the curious features of cell culture studies to explore the effect of FSS is that the response of ECs and PT cells is diametrically opposite. The formation of stress fibers, disruption of DPAB and redistribution of junction associated proteins follows a 'bumper car' as opposed to a 'junctional buttressing' model. This appears to be related to cell geometry, the difference between flat ECs and tall columnar PT cells. Numerous culture studies have been performed on bone cells, but the basic difficulty is that one cannot easily reproduce the *in vivo* environment of the lacunar-canalicular system. This makes it very difficult to distinguish the mechanical response of the cell body and its cell processes. The newly developed Stokesian fluid stimulus probe could prove to be a major advance in elucidating the localization of the stimulus and its transmission.[178]

There is a wide variety of signaling cascades that are initiated by fluid forces involved in the regulation of gene/protein expression. These have been most widely studied in ECs where Rho, FAK, Src, integrin regulated and KLF2 pathways have been extensively explored. These pathways lead to the release of signaling molecules such as NO, PGI_2 and Ca^{2+}. In bone cells the primary interest is in the mechano-signaling molecules ATP, PGE_2, NO and VEGF. The specific concern is bone maintenance and repair including osteoclast recruitment. In PT cells the primary interest is the induction of NHE3 and V-ATPase synthesis and their trafficking to the apical membrane at the base of the microvilli in the brush border. In the principal cells of the CCD primary cilia have received a heightened interest due to the role of $[Ca^{2+}]$ in polycystic kidney disease where the polycystins 1 and 2 are believed to be the key players in chemical regulation.

FUTURE DIRECTIONS

In this review we have tried to highlight some of the key unresolved issues that require further study in all three cell types. These issues are briefly summarized below.

Endothelial Cells

The molecular composition of the EGL and its proteoglycan composition has yet to be related to the ultrastructure observed in electronmicroscopy. This could help explain why there is such a large difference in EGL thickness between electron microscopic and *in vivo* intravital microscopic observations? One would also like to apply knowledge of the biochemical

TABLE 1. Summary comparison of ultrastructure and flow-dependent mechanisms in ECs, renal epithelial and osteocytes.

Ultrastructure	
ECs	Flat cells, apical surface covered by 0.5 μm thick EGL, effective pore size of 7 nm to sieve plasma proteins, shed in diabetes, inflammation and ischemia
PT cells	Tall cuboidal cells, apical surface covered with a brush border, 4000 microvilli/cell of 0.1 μm diameter and 2–3 μm height, single primary cilia
Principal cells CCD	Flat cells, central cilium, 9 + 0 microtubule structure, height 2–5 μm, stunted in polycystic kidney disease
Osteocytes	Dendritic processes, 20 μm length, central F-actin filament bundle, processes surrounded by 0.1 μm thick pericellular matrix, pore size 6–12 μm, process attached to canalicular wall, discrete punctate integrin attachment sites, primary cilia confined to lacuna near periosteal surface
FSS and mechanosensing of fluid flow	
ECs	FSS 1–3 Pa, sensed by core proteins in EGL, transmitted through core protein to underlying ACW creating a rotational moment on cadherin bonds at the level of the AJ, FSS attenuated by EGL and negligible at membrane surface
PT cells	FSS 0.1 Pa, sensed by microvilli, transmitted to ACW as a bending moment, stresses amplified 40 fold in ACW due to long lever arm
Principal cells CCD	FSS $\leq$ 0.05 Pa, sensed by long primary cilia, transmitted as a greatly amplified membrane stress at the base of basal body
Osteocytes	FSS 0.8–3 Pa at process membrane, fluid forces transmitted to central actin filament bundle by tensile forces on tethering filaments creating a hoop strain and greatly amplified axial strain in the vicinity of punctate integrin attachments
Relation of cell geometry to mechanosensitive response	
ECs	Flat cells elongate in response to flow to minimize the rotational moment on their DPAB and to stabilize their AJs
PT cells	Tall columnar cells with FSS 1/10 that of ECs, rotational moment similar to ECs due to long lever arm at base, brush border plays nearly same role as EGL in transmission of FSS to actin cytoskeleton
Principal cells CCD	Long primary cilium protrudes unobstructed into central part of the CCD which makes the CCD cilium an ideal antenna for detecting very small changes in flow
Osteocytes	Processes are stiff compared to their cell body, special attachments are required to greatly amplify whole tissue strains at the cellular level to initiate cellular signaling, drag forces on pericellular matrix components create membrane strains not FSS, primary cilium believed to be chemical but not flow sensor
Cytoskeletal, junctional and focal adhesion reorganization in response to FSS in culture	
ECs	Formation of basal stress fibers, disruption of the DPAB, redistribution of junction associated proteins ZO-1 and Cx43, and focal adhesion associated protein vinculin, "bumper car" model[159]
PT cells	Basal stress fibers present in static control disappear, formation of AJs and tight junctions, relocation of focal adhesion proteins vinculin and paxillin to basal membrane, "junctional buttressing" model[40]
Principal cells CCD	Cytoskeletal, junctional and focal adhesion response to FSS has not been studied
Osteocytes	Cytoskeletal response to FSS has not been studied, junction associated proteins ZO-1 and Cx43 redistribute in response to FSS
Downstream signaling	
ECs	Modulation of gene/protein expression (Rho, FAK, Src, integrins, KLF2), release of mechanosig naling molecules PGI_2, NO, and Ca^{2+}
PT cells	Induction of NHE3 and V-ATPase synthesis, luminal protein trafficking to the apical plasma membrane
Principal cells CCD	Release of $[Ca^{2+}]_i$ through polycystin-2 which is activated by conformation changes of polycystin-1 that transduce the mechanical signal into a chemical response
Osteocytes	Transient $[Ca^{2+}]_i$, increase, release of mechanosignaling molecules ATP, PGE_2, NO, and VEGF

PT, proximal tubule; CCD, cortical collecting duct; EC, endothelial cell; EGL, endothelial glycocalyx layer; FSS, fluid shear stress; ACW, actin cortical web; DPAB, dense peripheral actin band; AJ, adherens junction; NO, nitric oxide; PGI_2 and PGE_2, prostaglandin I_2 and E_2; VEGF, vascular endothelial growth factor; $[Ca^{2+}]_i$, intracellular calcium.

composition of the EGL in order to better understand enzymatic degradation processes in the EGL. This will shed light on why the EGL has a different role in regulating FSS-induced NO and PGI_2 release. For example, why does partial removal of selected EGL components completely block FSS-induced NO release, but not PGI_2 release?[49,65,114] A third issue is to determine the importance of an intact EGL in the initiation and maintenance of tethered leukocyte rolling and attachment. What role does the EGL play during inflammation? Does the EGL have to be degraded for leukocytes to attach and is attachment restricted to postcapillary venules.[187]

Renal Epithelial Cells

There are two critical issues in the nephron PT which warrant further study: the coupling and cross

talk between membrane transport proteins at the apical and basolateral aspects of brush border cells, and the cytoskeletal signaling associated with transporter trafficking and expression. In addition, the role of primary cilia in PT cells needs to be investigated. One wants to know whether the primary cilia function as part of mechanosensory machinery or act as a vestigial apparatus. As for the distal nephron, important unresolved issues are to clarify the molecular basis for the intercalated cell response to FSS, which was not discussed in this review, and to unravel the components of the signaling pathways activated by flow in addition to the Ca^{2+} response described in this review.

Dendritic Cells (Osteocytes)

A central issue that requires further study is to elucidate whether structural differences in the osteocyte cell body and processes play a role in transmission of FSS-induced intracellular signalings. Recent studies by Burra *et al.*[19] using a transwell filter system to differentiate cell body and cell process responses to flow demonstrate that integrin attachments along osteocyte dendritic processes are indeed mechanotransducers. In addition, as mentioned in "Dendritic Cells (Osteocytes)" section a new tool (a novel Stokesian fluid stimulus probe[178]) that allows localized pN level force stimulation and intracellular response acquisition has been developed. Another key issue that still needs to be addressed is to verify whether integrins (β_1, β_3 integrins) play a pivotal role in the initiation of mechanosignaling as suggested by *in vivo* findings.[103] Recently, β_1 integrin has been shown to play a role in FSS-induced PGE_2 release in osteocytes.[92] Moreover, it is also essential to identify the pathways that are involved in release of ATP and PGE_2 and which triggers the release of the other. Presently, there are conflicting results, one demonstrating that the Cx43 hemichannel serves as the channel assisting release of either PGE_2[23] or ATP release, while the other indicates that $P2X_7R$ serves as a pathway for PGE_2 release.[57,91]

Determining these issues will not only elucidate mechanotransduction mechanisms in all three cell types but also will help develop new therapeutic approaches to prevent vascular, renal and bone diseases.

ACKNOWLEDGMENTS

This work was supported by National Institute of Health grants HL44485 (endothelium), DK-62289 (renal), and AR48699 and AR057139 (bone).

REFERENCES

[1]Adachi, T., Y. Aonuma, M. Tanaka, M. Hojo, T. Takano-Yamamoto, and H. Kamioka. Calcium response in single osteocytes to locally applied mechanical stimulus: differences in cell process and cell body. *J. Biomech.* 42:1989–1995, 2009.

[2]Adamson, R. H., and G. Clough. Plasma proteins modify the endothelial cell glycocalyx of frog mesenteric microvessels. *J. Physiol.* 445:473–486, 1992.

[3]Adamson, R. H., J. F. Lenz, X. Zhang, G. N. Adamson, S. Weinbaum, and F. E. Curry. Oncotic pressures opposing filtration across non-fenestrated rat microvessels. *J. Physiol.* 557:889–907, 2004.

[4]Akst, J. Full speed ahead: physical forces acting in and around cells are fast—and making waves in the world of molecular biology. *Scientist* 23:26–32, 2009.

[5]Alenghat, F. J., S. M. Nauli, R. Kolb, J. Zhou, and D. E. Ingber. Global cytoskeletal control of mechanotransduction in kidney epithelial cells. *Exp. Cell Res.* 301:23–30, 2004.

[6]Alford, A. I., C. R. Jacobs, and H. J. Donahue. Oscillating fluid flow regulates gap junction communication in osteocytic MLO-Y4 cells by an ERK1/2 MAP kinase-dependent mechanism small star, filled. *Bone* 33:64–70, 2003.

[7]Anderson, C. T., A. B. Castillo, S. A. Brugmann, J. A. Helms, C. R. Jacobs, and T. Stearns. Primary cilia: cellular sensors for the skeleton. *Anat. Rec. (Hoboken)* 291:1074–1078, 2008.

[8]Ayasaka, N., T. Kondo, T. Goto, M. A. Kido, E. Nagata, and T. Tanaka. Differences in the transport systems between cementocytes and osteocytes in rats using microperoxidase as a tracer. *Arch. Oral Biol.* 37:363–369, 1992.

[9]Bakker, A. D., V. C. Silva, R. Krishnan, R. G. Bacabac, M. E. Blaauboer, R. A. Marcantonio, J. A. Cirelli, J. Klein-Nulend, and Y. C. Lin. Tumor necrosis factor alpha and interleukin-1beta modulate calcium and nitric oxide signaling in mechanically stimulated osteocytes. *Arthritis Rheum.* 60:3336–3345, 2009.

[10]Bartles, J. R., L. Zheng, A. Li, A. Wierda, and B. Chen. Small espin: a third actin-bundling protein and potential forked protein ortholog in brush border microvilli. *J. Cell Biol.* 143:107–119, 1998.

[11]Bass, M. D., and M. J. Humphries. Cytoplasmic interactions of syndecan-4 orchestrate adhesion receptor and growth factor receptor signalling. *Biochem. J.* 368:1–15, 2002.

[12]Bates, J. M., J. Akerlund, E. Mittge, and K. Guillemin. Intestinal alkaline phosphatase detoxifies lipopolysaccharide and prevents inflammation in zebrafish in response to the gut microbiota. *Cell Host Microbe* 2:371–382, 2007.

[13]Baumgartner, W., P. Hinterdorfer, W. Ness, A. Raab, D. Vestweber, H. Schindler, and D. Drenckhahn. Cadherin interaction probed by atomic force microscopy. *Proc. Natl Acad. Sci. USA* 97:4005–4010, 2000.

[14]Broekhuizen, L. N., B. A. Lemkes, H. L. Mooij, M. C. Meuwese, H. Verberne, F. Holleman, R. O. Schlingemann, M. Nieuwdorp, E. S. Stroes, and H. Vink. Effect of sulodexide on endothelial glycocalyx and vascular permeability in patients with type 2 diabetes mellitus. *Diabetologia* 53:2646–2655, 2010.

[15]Burg, M. B., and J. Orloff. Control of fluid absorption in the renal proximal tubule. *J. Clin. Invest.* 47:2016–2024, 1968.

[16]Burger, E. H., J. Klein-Nulend, and T. H. Smit. Strain-derived canalicular fluid flow regulates osteoclast activity in

a remodelling osteon—a proposal. *J. Biomech.* 36:1453–1459, 2003.
[17]Burr, D. B., C. Milgrom, D. Fyhrie, M. Forwood, M. Nyska, A. Finestone, S. Hoshaw, E. Saiag, and A. Simkin. In vivo measurement of human tibial strains during vigorous activity. *Bone* 18:405–410, 1996.
[18]Burra, S., and J. X. Jiang. Connexin 43 hemichannel opening associated with Prostaglandin E(2) release is adaptively regulated by mechanical stimulation. *Commun. Integr. Biol.* 2:239–240, 2009.
[19]Burra, S., D. P. Nicolella, W. L. Francis, C. J. Freitas, N. J. Mueschke, K. Poole, and J. X. Jiang. Dendritic processes of osteocytes are mechanotransducers that induce the opening of hemichannels. *Proc. Natl Acad. Sci. USA* 107:13648–13653, 2010.
[20]Chappell, D., M. Jacob, K. Hofmann-Kiefer, M. Rehm, U. Welsch, P. Conzen, and B. F. Becker. Antithrombin reduces shedding of the endothelial glycocalyx following ischaemia/reperfusion. *Cardiovasc. Res.* 83:388–396, 2009.
[21]Cheng, B. X., Y. Kato, S. Zhao, J. Luo, E. Sprague, L. F. Bonewald, and J. X. Jiang. PGE(2) is essential for gap junction-mediated intercellular communication between osteocyte-like MLO-Y4 cells in response to mechanical strain. *Endocrinology* 142:3464–3473, 2001.
[22]Cheng, B., S. Zhao, J. Luo, E. Sprague, L. F. Bonewald, and J. X. Jiang. Expression of functional gap junctions and regulation by fluid flow in osteocyte-like MLO-Y4 cells. *J. Bone Miner. Res.* 16:249–259, 2001.
[23]Cherian, P. P., A. J. Siller-Jackson, S. Gu, X. Wang, L. F. Bonewald, E. Sprague, and J. X. Jiang. Mechanical strain opens connexin 43 hemichannels in osteocytes: a novel mechanism for the release of prostaglandin. *Mol. Biol. Cell* 16:3100–3106, 2005.
[24]Cheung, W. Y., C. Liu, R. M. Tonelli-Zasarsky, C. A. Simmons, and L. You. Osteocyte apoptosis is mechanically regulated and induces angiogenesis in vitro. *J. Orthop. Res.* 29:523–530, 2011.
[25]Chien, S. Mechanotransduction and endothelial cell homeostasis: the wisdom of the cell. *Am. J. Physiol. Heart Circ. Physiol.* 292:H1209–H1224, 2007.
[26]Ciani, C., S. B. Doty, and S. P. Fritton. Mapping bone interstitial fluid movement: displacement of ferritin tracer during histological processing. *Bone* 37:379–387, 2005.
[27]Coluccio, L. M. Identification of the microvillar 110-kDa calmodulin complex (myosin-1) in kidney. *Eur. J. Cell Biol.* 56:286–294, 1991.
[28]Cowin, S. C. Bone poroelasticity. *J. Biomech.* 32:217–238, 1999.
[29]Damiano, E. R. The effect of the endothelial-cell glycocalyx on the motion of red blood cells through capillaries. *Microvasc. Res.* 55:77–91, 1998.
[30]Damiano, E. R., and T. M. Stace. A mechano-electrochemical model of radial deformation of the capillary glycocalyx. *Biophys. J.* 82:1153–1175, 2002.
[31]Davies, P. F. Flow-mediated endothelial mechanotransduction. *Physiol. Rev.* 75:519–560, 1995.
[32]del Alamo, J. C., G. N. Norwich, Y. S. Li, J. C. Lasheras, and S. Chien. Anisotropic rheology and directional mechanotransduction in vascular endothelial cells. *Proc. Natl Acad. Sci. USA* 105:15411–15416, 2008.
[33]Dillaman, R. M. Movement of ferritin in the 2-day-old chick femur. *Anat. Rec.* 209:445–453, 1984.
[34]Discher, D., C. Dong, J. J. Fredberg, F. Guilak, D. Ingber, P. Janmey, R. D. Kamm, G. W. Schmid-Schonbein, and S. Weinbaum. Biomechanics: cell research and applications for the next decade. *Ann. Biomed. Eng.* 37:847–859, 2009.
[35]Discher, D. E., P. Janmey, and Y. L. Wang. Tissue cells feel and respond to the stiffness of their substrate. *Science* 310:1139–1143, 2005.
[36]Donahue, H. J. Gap junctions and biophysical regulation of bone cell differentiation. *Bone* 26:417–422, 2000.
[37]Doty, S. B., and B. H. Schofield. Metabolic and structural changes within osteocytes of rat bone. In: Calcium, Parathyroid Hormone and the Calcitonins, edited by R. V. Talmage, and P. L. Munson. Amsterdam: Elsevier, 1972, pp. 353–364.
[38]Du, Z., Y. Duan, Q. Yan, A. M. Weinstein, S. Weinbaum, and T. Wang. Mechanosensory function of microvilli of the kidney proximal tubule. *Proc. Natl Acad. Sci. USA* 101:13068–13073, 2004.
[39]Du, Z., Q. Yan, Y. Duan, S. Weinbaum, A. M. Weinstein, and T. Wang. Axial flow modulates proximal tubule NHE3 and H-ATPase activities by changing microvillus bending moments. *Am. J. Physiol. Renal Physiol.* 290:F289–F296, 2006.
[40]Duan, Y., N. Gotoh, Q. Yan, Z. Du, A. M. Weinstein, T. Wang, and S. Weinbaum. Shear-induced reorganization of renal proximal tubule cell actin cytoskeleton and apical junctional complexes. *Proc. Natl Acad. Sci. USA* 105:11418–11423, 2008.
[41]Duan, Y., A. M. Weinstein, S. Weinbaum, and T. Wang. Shear stress-induced changes of membrane transporter localization and expression in mouse proximal tubule cells. *Proc. Natl Acad. Sci. USA* 107:21860–21865, 2010.
[42]Engler, A. J., S. Sen, H. L. Sweeney, and D. E. Discher. Matrix elasticity directs stem cell lineage specification. *Cell* 126:677–689, 2006.
[43]Essig, M., F. Terzi, M. Burtin, and G. Friedlander. Mechanical strains induced by tubular flow affect the phenotype of proximal tubular cells. *Am. J. Physiol. Renal Physiol.* 281:F751–F762, 2001.
[44]Evans, E., and K. Ritchie. Dynamic strength of molecular adhesion bonds. *Biophys. J.* 72:1541–1555, 1997.
[45]Federman, M., and G. Nichols, Jr. Bone cell cilia: vestigial or functional organelles? *Calcif. Tissue Res.* 17:81–85, 1974.
[46]Fehon, R. G., A. I. McClatchey, and A. Bretscher. Organizing the cell cortex: the role of ERM proteins. *Nat. Rev. Mol. Cell Biol.* 11:276–287, 2010.
[47]Feng, J., and S. Weinbaum. Lubrication theory in highly compressible porous media: the mechanics of skiing, from red cells to humans. *J. Fluid Mech.* 422:281–317, 2000.
[48]Flaherty, J. T., J. E. Pierce, V. J. Ferrans, D. J. Patel, W. K. Tucker, and D. L. Fry. Endothelial nuclear patterns in the canine arterial tree with particular reference to hemodynamic events. *Circ. Res.* 30:23–33, 1972.
[49]Florian, J. A., J. R. Kosky, K. Ainslie, Z. Pang, R. O. Dull, and J. M. Tarbell. Heparan sulfate proteoglycan is a mechanosensor on endothelial cells. *Circ. Res.* 93:e136–e142, 2003.
[50]Fornells, P., J. M. Garcia-Aznar, and M. Doblare. A finite element dual porosity approach to model deformation-induced fluid flow in cortical bone. *Ann. Biomed. Eng.* 35:1687–1698, 2007.
[51]Frangos, J. A., S. G. Eskin, L. V. McIntire, and C. L. Ives. Flow effects on prostacyclin production by cultured human endothelial cells. *Science* 227:1477–1479, 1985.
[52]Fritton, S. P., K. J. McLeod, and C. T. Rubin. Quantifying the strain history of bone: spatial uniformity and self-similarity of low-magnitude strains. *J. Biomech.* 33:317–325, 2000.

[53]Fritton, S. P., and S. Weinbaum. Fluid and solute transport in bone: flow-induced mechanotransduction. *Annu. Rev. Fluid Mech*. 41:347–374, 2009.
[54]Fu, B. M., B. Chen, and W. Chen. An electrodiffusion model for effects of surface glycocalyx layer on microvessel permeability. *Am. J. Physiol. Heart Circ. Physiol*. 284:H1240–H1250, 2003.
[55]Galbraith, C. G., R. Skalak, and S. Chien. Shear stress induces spatial reorganization of the endothelial cell cytoskeleton. *Cell Motil. Cytoskeleton* 40:317–330, 1998.
[56]Gao, L., and H. H. Lipowsky. Composition of the endothelial glycocalyx and its relation to its thickness and diffusion of small solutes. *Microvasc. Res*. 80:394–401, 2010.
[57]Genetos, D. C., C. J. Kephart, Y. Zhang, C. E. Yellowley, and H. J. Donahue. Oscillating fluid flow activation of gap junction hemichannels induces ATP release from MLO-Y4 osteocytes. *J. Cell. Physiol*. 212:207–214, 2007.
[58]Goldberg, R. F., W. G. Austen, Jr., X. Zhang, G. Munene, G. Mostafa, S. Biswas, M. McCormack, K. R. Eberlin, J. T. Nguyen, H. S. Tatlidede, H. S. Warren, S. Narisawa, J. L. Millan, and R. A. Hodin. Intestinal alkaline phosphatase is a gut mucosal defense factor maintained by enteral nutrition. *Proc. Natl Acad. Sci. USA* 105:3551–3556, 2008.
[59]Goldfinger, L. E., E. Tzima, R. Stockton, W. B. Kiosses, K. Kinbara, E. Tkachenko, E. Gutierrez, A. Groisman, P. Nguyen, S. Chien, and M. H. Ginsberg. Localized alpha4 integrin phosphorylation directs shear stress-induced endothelial cell alignment. *Circ. Res*. 103:177–185, 2008.
[60]Goulet, G. C., D. Coombe, R. J. Martinuzzi, and R. F. Zernicke. Poroelastic evaluation of fluid movement through the lacunocanalicular system. *Ann. Biomed. Eng*. 37:1390–1402, 2009.
[61]Guo, P., A. M. Weinstein, and S. Weinbaum. A hydrodynamic mechanosensory hypothesis for brush border microvilli. *Am. J. Physiol. Renal Physiol*. 279:F698–F712, 2000.
[62]Gururaja, S., H. J. Kim, C. C. Swan, R. A. Brand, and R. S. Lakes. Modeling deformation-induced fluid flow in cortical bone's canalicular-lacunar system. *Ann. Biomed. Eng*. 33:7–25, 2005.
[63]Han, Y. F., S. C. Cowin, M. B. Schaffler, and S. Weinbaum. Mechanotransduction and strain amplification in osteocyte cell processes. *Proc. Natl Acad. Sci. USA* 101:16689–16694, 2004.
[64]Han, Y., S. Weinbaum, J. A. E. Spaan, and H. Vink. Large-deformation analysis of the elastic recoil of fibre layers in a Brinkman medium with application to the endothelial glycocalyx. *J. Fluid Mech*. 554:217–235, 2006.
[65]Hecker, M., A. Mulsch, E. Bassenge, and R. Busse. Vasoconstriction and increased flow: two principal mechanisms of shear stress-dependent endothelial autacoid release. *Am. J. Physiol*. 265:H828–H833, 1993.
[66]Heinrich, V., and C. Ounkomol. Force versus axial deflection of pipette-aspirated closed membranes. *Biophys. J*. 93:363–372, 2007.
[67]Henry, C. B., and B. R. Duling. Permeation of the luminal capillary glycocalyx is determined by hyaluronan. *Am. J. Physiol*. 277:H508–H514, 1999.
[68]Herzog, F. A., J. Geraedts, D. Hoey, and C. R. Jacobs. A mathematical approach to study the bending behavior of the primary cilium. In: Bioengineering Conference, Proceedings of the 2010 IEEE 36th Annual Northeast, New York, NY, 2010.
[69]Hildebrandt, F., and E. Otto. Cilia and centrosomes: a unifying pathogenic concept for cystic kidney disease? *Nat. Rev. Genet*. 6:928–940, 2005.
[70]Hsu, P. P., S. Li, Y. S. Li, S. Usami, A. Ratcliffe, X. Wang, and S. Chien. Effects of flow patterns on endothelial cell migration into a zone of mechanical denudation. *Biochem. Biophys. Res. Commun*. 285:751–759, 2001.
[71]Hu, S., L. Eberhard, J. Chen, J. C. Love, J. P. Butler, J. J. Fredberg, G. M. Whitesides, and N. Wang. Mechanical anisotropy of adherent cells probed by a three-dimensional magnetic twisting device. *Am. J. Physiol. Cell Physiol*. 287:C1184–C1191, 2004.
[72]Hu, X., and S. Weinbaum. A new view of starling's hypothesis at the microstructural level. *Microvasc. Res*. 58:281–304, 1999.
[73]Ihrcke, N. S., L. E. Wrenshall, B. J. Lindman, and J. L. Platt. Role of heparan sulfate in immune system-blood vessel interactions. *Immunol. Today* 14:500–505, 1993.
[74]Ingber, D. E., and I. Tensegrity. Cell structure and hierarchical systems biology. *J. Cell Sci*. 116:1157–1173, 2003.
[75]Jacobs, C. R., S. Temiyasathit, and A. B. Castillo. Osteocyte mechanobiology and pericellular mechanics. *Annu. Rev. Biomed. Eng*. 12:369–400, 2010.
[76]Kitase, Y., L. Barragan, H. Qing, S. Kondoh, J. X. Jiang, M. L. Johnson, and L. F. Bonewald. Mechanical induction of PGE2 in osteocytes blocks glucocorticoid-induced apoptosis through both the beta-catenin and PKA pathways. *J. Bone Miner. Res*. 25:2381–2392, 2010.
[77]Klein-Nulend, J., C. M. Semeins, N. E. Ajubi, P. J. Nijweide, and E. H. Burger. Pulsating fluid flow increases nitric oxide (NO) synthesis by osteocytes but not periosteal fibroblasts—correlation with prostaglandin upregulation. *Biochem. Biophys. Res. Commun*. 217:640–648, 1995.
[78]Klein-Nulend, J., A. van der Plas, C. M. Semeins, N. E. Ajubi, J. A. Frangos, P. J. Nijweide, and E. H. Burger. Sensitivity of osteocytes to biomechanical stress in vitro. *FASEB J*. 9:441–445, 1995.
[79]Knothe Tate, M. L., and U. Knothe. An ex vivo model to study transport processes and fluid flow in loaded bone. *J. Biomech*. 33:247–254, 2000.
[80]Knothe Tate, M. L., R. Steck, M. R. Forwood, and P. Niederer. In vivo demonstration of load-induced fluid flow in the rat tibia and its potential implications for processes associated with functional adaptation. *J. Exp. Biol*. 203(Pt 18):2737–2745, 2000.
[81]Knothe Tate, M. L., P. Niederer, and U. Knothe. In vivo tracer transport through the lacunocanalicular system of rat bone in an environment devoid of mechanical loading. *Bone* 22:107–117, 1998.
[82]Kotsis, F., R. Nitschke, M. Doerken, G. Walz, and E. W. Kuehn. Flow modulates centriole movements in tubular epithelial cells. *Pflugers Arch*. 456:1025–1035, 2008.
[83]Kuchan, M. J., and J. A. Frangos. Role of calcium and calmodulin in flow-induced nitric oxide production in endothelial cells. *Am. J. Physiol*. 266:C628–C636, 1994.
[84]Kuchan, M. J., H. Jo, and J. A. Frangos. Role of G proteins in shear stress-mediated nitric oxide production by endothelial cells. *Am. J. Physiol*. 267:C753–C758, 1994.
[85]Kwon, R. Y., D. R. Meays, W. J. Tang, and J. A. Frangos. Microfluidic enhancement of intramedullary pressure increases interstitial fluid flow and inhibits bone loss in hindlimb suspended mice. *J. Bone Miner. Res*. 25:1798–1807, 2010.
[86]Kwon, R. Y., and J. A. Frangos. Quantification of lacunar-canalicular interstitial fluid flow through computational modeling of fluorescence recovery after photobleaching. *Cell Mol. Bioeng*. 3:296–306, 2010.

[87]Kwon, R. Y., S. Temiyasathit, P. Tummala, C. C. Quah, and C. R. Jacobs. Primary cilium-dependent mechanosensing is mediated by adenylyl cyclase 6 and cyclic AMP in bone cells. *FASEB J.* 24:2859–2868, 2010.
[88]Lamprecht, G., E. J. Weinman, and C. H. Yun. The role of NHERF and E3KARP in the cAMP-mediated inhibition of NHE3. *J. Biol. Chem.* 273:29972–29978, 1998.
[89]Li, S., P. Butler, Y. Wang, Y. Hu, D. C. Han, S. Usami, J. L. Guan, and S. Chien. The role of the dynamics of focal adhesion kinase in the mechanotaxis of endothelial cells. *Proc. Natl Acad. Sci. USA* 99:3546–3551, 2002.
[90]Li, Y. S., J. H. Haga, and S. Chien. Molecular basis of the effects of shear stress on vascular endothelial cells. *J. Biomech.* 38:1949–1971, 2005.
[91]Li, J., D. Liu, H. Z. Ke, R. L. Duncan, and C. H. Turner. The P2X7 nucleotide receptor mediates skeletal mechanotransduction. *J. Biol. Chem.* 280:42952–42959, 2005.
[92]Litzenberger, J. B., J. B. Kim, P. Tummala, and C. R. Jacobs. Beta1 integrins mediate mechanosensitive signaling pathways in osteocytes. *Calcif. Tissue Int.* 86:325–332, 2010.
[93]Liu, W., S. Xu, C. Woda, P. Kim, S. Weinbaum, and L. M. Satlin. Effect of flow and stretch on the $[Ca^{2+}]$i response of principal and intercalated cells in cortical collecting duct. *Am. J. Physiol. Renal Physiol.* 285:F998–F1012, 2003.
[94]Lopez-Quintero, S. V., R. Amaya, M. Pahakis, and J. M. Tarbell. The endothelial glycocalyx mediates shear-induced changes in hydraulic conductivity. *Am. J. Physiol. Heart Circ. Physiol.* 296:H1451–H1456, 2009.
[95]Luft, J. H. Fine structures of capillary and endocapillary layer as revealed by ruthenium red. *Fed. Proc.* 25:1773–1783, 1966.
[96]Maddox, D. A., S. M. Fortin, A. Tartini, W. D. Barnes, and F. J. Gennari. Effect of acute changes in glomerular filtration rate on Na^+/H^+ exchange in rat renal cortex. *J. Clin. Invest.* 89:1296–1303, 1992.
[97]Mak, A. F. T., L. Qin, L. K. Hung, C. W. Cheng, and C. F. Tin. A histomorphometric observation of flows in cortical bone under dynamic loading. *Microvasc. Res.* 59:290–300, 2000.
[98]Malone, A. M., N. N. Batra, G. Shivaram, R. Y. Kwon, L. You, C. H. Kim, J. Rodriguez, K. Jair, and C. R. Jacobs. The role of actin cytoskeleton in oscillatory fluid flow-induced signaling in MC3T3-E1 osteoblasts. *Am. J. Physiol. Cell Physiol.* 292:C1830–C1836, 2007.
[99]Maunsbach, A. Ultrastructure of the proximal tubule. In: Handbook of Physiology, Section 8: Renal Physiology, edited by J. Orloff, and R. Berliner. Washington, DC: Am Physiol Soc, 1973, pp. 31–79.
[100]McConnell, R. E., J. N. Higginbotham, D. A. Shifrin, Jr., D. L. Tabb, R. J. Coffey, and M. J. Tyska. The enterocyte microvillus is a vesicle-generating organelle. *J. Cell Biol.* 185:1285–1298, 2009.
[101]McDonough, A. A. Mechanisms of proximal tubule sodium transport regulation that link extracellular fluid volume and blood pressure. *Am. J. Physiol. Regul. Integr. Comp. Physiol.* 298:R851–R861, 2010.
[102]McNamara, L. M., A. G. Ederveen, C. G. Lyons, C. Price, M. B. Schaffler, H. Weinans, and P. J. Prendergast. Strength of cancellous bone trabecular tissue from normal, ovariectomized and drug-treated rats over the course of ageing. *Bone* 39:392–400, 2006.
[103]McNamara, L. M., R. J. Majeska, S. Weinbaum, V. Friedrich, and M. B. Schaffler. Primary cilia in bone: few in number and restricted in their location. *Anat. Rec.* 2011 (accepted).
[104]McNamara, L. M., R. J. Majeska, S. Weinbaum, V. Friedrich, and M. B. Schaffler. Attachment of osteocyte cell processes to the bone matrix. *Anat. Rec. (Hoboken)* 292:355–363, 2009.
[105]Michel, C. C. Starling: the formulation of his hypothesis of microvascular fluid exchange and its significance after 100 years. *Exp. Physiol.* 82:1–30, 1997.
[106]Montgomery, R. J., B. D. Sutker, J. T. Bronk, S. R. Smith, and P. J. Kelly. Interstitial fluid flow in cortical bone. *Microvasc. Res.* 35:295–307, 1988.
[107]Mulivor, A. W., and H. H. Lipowsky. Inflammation- and ischemia-induced shedding of venular glycocalyx. *Am. J. Physiol. Heart Circ. Physiol.* 286:H1672–H1680, 2004.
[108]Nauli, S. M., F. J. Alenghat, Y. Luo, E. Williams, P. Vassilev, X. Li, A. E. H. Elia, W. Lu, E. M. Brown, S. J. Quinn, D. E. Ingber, and J. Zhou. Polycystins 1 and 2 mediate mechanosensation in the primary cilium of kidney cells. *Nat. Genet.* 33:129–137, 2003.
[109]Nieuwdorp, M., T. W. van Haeften, M. C. Gouverneur, H. L. Mooij, M. H. van Lieshout, M. Levi, J. C. Meijers, F. Holleman, J. B. Hoekstra, H. Vink, J. J. Kastelein, and E. S. Stroes. Loss of endothelial glycocalyx during acute hyperglycemia coincides with endothelial dysfunction and coagulation activation in vivo. *Diabetes* 55:480–486, 2006.
[110]Noonan, K. J., J. W. Stevens, R. Tammi, M. Tammi, J. A. Hernandez, and R. J. Midura. Spatial distribution of CD44 and hyaluronan in the proximal tibia of the growing rat. *J. Orthop. Res.* 14:573–581, 1996.
[111]Orci, L., F. Humbert, D. Brown, and A. Perrelet. Membrane ultrastructure in urinary tubules. *Int. Rev. Cytol.* 73:183–242, 1981.
[112]Pahakis, M. Y., J. R. Kosky, R. O. Dull, and J. M. Tarbell. The role of endothelial glycocalyx components in mechanotransduction of fluid shear stress. *Biochem. Biophys. Res. Commun.* 355:228–233, 2007.
[113]Piekarski, K., and M. Munro. Transport mechanism operating between blood supply and osteocytes in long bones. *Nature* 269:80–82, 1977.
[114]Pohl, U., K. Herlan, A. Huang, and E. Bassenge. EDRF-mediated shear-induced dilation opposes myogenic vasoconstriction in small rabbit arteries. *Am. J. Physiol.* 261:H2016–H2023, 1991.
[115]Ponik, S. M., J. W. Triplett, and F. M. Pavalko. Osteoblasts and osteocytes respond differently to oscillatory and unidirectional fluid flow profiles. *J. Cell. Biochem.* 100:794–807, 2007.
[116]Praetorius, H. A., and K. R. Spring. Bending the MDCK cell primary cilium increases intracellular calcium. *J. Membr. Biol.* 184:71–79, 2001.
[117]Praetorius, H. A., and K. R. Spring. Removal of the MDCK cell primary cilium abolishes flow sensing. *J. Membr. Biol.* 191:69–76, 2003.
[118]Praetorius, H. A., and K. R. Spring. A physiological view of the primary cilium. *Annu. Rev. Physiol.* 67:515–529, 2005.
[119]Preisig, P. A. Luminal flow rate regulates proximal tubule H-HCO_3 transporters. *Am. J. Physiol.* 262:F47–F54, 1992.
[120]Price, C., X. Zhou, W. Li, and L. Wang. Real-time measurement of solute transport within the lacunar-canalicular system of mechanically loaded bone: direct evidence for load-induced fluid flow. *J. Bone Miner. Res.* 26:277–285, 2011.
[121]Pries, A. R., T. W. Secomb, and P. Gaehtgens. The endothelial surface layer. *Pflugers Arch.* 440:653–666, 2000.

[122]Pries, A. R., T. W. Secomb, T. Gessner, M. B. Sperandio, J. F. Gross, and P. Gaehtgens. Resistance to blood flow in microvessels in vivo. *Circ. Res.* 75:904–915, 1994.
[123]Qin, Y. X., T. Kaplan, A. Saldanha, and C. Rubin. Fluid pressure gradients, arising from oscillations in intramedullary pressure, is correlated with the formation of bone and inhibition of intracortical porosity. *J. Biomech.* 36:1427–1437, 2003.
[124]Qin, L., A. T. Mak, C. W. Cheng, L. K. Hung, and K. M. Chan. Histomorphological study on pattern of fluid movement in cortical bone in goats. *Anat. Rec.* 255:380–387, 1999.
[125]Rapraeger, A., M. Jalkanen, E. Endo, J. Koda, and M. Bernfield. The cell surface proteoglycan from mouse mammary epithelial cells bears chondroitin sulfate and heparan sulfate glycosaminoglycans. *J. Biol. Chem.* 260:11046–11052, 1985.
[126]Reich, K. M., and J. A. Frangos. Effect of flow on prostaglandin E2 and inositol trisphosphate levels in osteoblasts. *Am. J. Physiol.* 261:C428–C432, 1991.
[127]Reilly, G. C., T. R. Haut, C. E. Yellowley, H. J. Donahue, and C. R. Jacobs. Fluid flow induced PGE_2 release by bone cells is reduced by glycocalyx degradation whereas calcium signals are not. *Biorheology* 40:591–603, 2003.
[128]Resnick, A. Use of optical tweezers to probe epithelial mechanosensation. *J. Biomed. Opt.* 15:015005, 2010.
[129]Resnick, A., and U. Hopfer. Force-response considerations in ciliary mechanosensation. *Biophys. J.* 93:1380–1390, 2007.
[130]Rodman, J. S., M. Mooseker, and M. G. Farquhar. Cytoskeletal proteins of the rat kidney proximal tubule brush border. *Eur. J. Cell Biol.* 42:319–327, 1986.
[131]Rostgaard, J., and K. Qvortrup. Electron microscopic demonstrations of filamentous molecular sieve plugs in capillary fenestrae. *Microvasc. Res.* 53:1–13, 1997.
[132]Roth, K. E., C. L. Rieder, and S. S. Bowser. Flexible-substratum technique for viewing cells from the side: some in vivo properties of primary (9 + 0) cilia in cultured kidney epithelia. *J. Cell. Sci.* 89(Pt 4):457–466, 1988.
[133]Rydholm, S., G. Zwartz, J. M. Kowalewski, P. Kamali-Zare, T. Frisk, and H. Brismar. Mechanical properties of primary cilia regulate the response to fluid flow. *Am. J. Physiol. Renal Physiol.* 298:F1096–F1102, 2010.
[134]Santos, A., A. D. Bakker, B. Zandieh-Doulabi, J. M. de Blieck-Hogervorst, and J. Klein-Nulend. Early activation of the beta-catenin pathway in osteocytes is mediated by nitric oxide, phosphatidyl inositol-3 kinase/Akt, and focal adhesion kinase. *Biochem. Biophys. Res. Commun.* 391:364–369, 2010.
[135]Santos, A., A. D. Bakker, B. Zandieh-Doulabi, C. M. Semeins, and J. Klein-Nulend. Pulsating fluid flow modulates gene expression of proteins involved in Wnt signaling pathways in osteocytes. *J. Orthop. Res.* 27:1280–1287, 2009.
[136]Satlin, L. M., and L. G. Palmer. Apical K^+ conductance in maturing rabbit principal cell. *Am. J. Physiol.* 272:F397–F404, 1997.
[137]Schnermann, J., M. Wahl, G. Liebau, and H. Fischbach. Balance between tubular flow rate and net fluid reabsorption in the proximal convolution of the rat kidney I. Dependency of reabsorptive net fluid flux upon proximal tubular surface area at spontaneous variations of filtration rate. *Pflugers Arch.* 304:90–103, 1968.
[138]Schwartz, E. A., M. L. Leonard, R. Bizios, and S. S. Bowser. Analysis and modeling of the primary cilium bending response to fluid shear. *Am. J. Physiol.* 272:F132–F138, 1997.
[139]Secomb, T. W., R. Hsu, and A. R. Pries. A model for red blood cell motion in glycocalyx-lined capillaries. *Am. J. Physiol.* 274:H1016–H1022, 1998.
[140]Secomb, T. W., R. Hsu, and A. R. Pries. Effect of the endothelial surface layer on transmission of fluid shear stress to endothelial cells. *Biorheology* 38:143–150, 2001.
[141]Secomb, T. W., R. Hsu, and A. R. Pries. Motion of red blood cells in a capillary with an endothelial surface layer: effect of flow velocity. *Am. J. Physiol. Heart Circ. Physiol.* 281:H629–H636, 2001.
[142]Shyy, J. Y., and S. Chien. Role of integrins in endothelial mechanosensing of shear stress. *Circ. Res.* 91:769–775, 2002.
[143]Simon, A., and M. C. Durrieu. Strategies and results of atomic force microscopy in the study of cellular adhesion. *Micron* 37:1–13, 2006.
[144]Squire, J. M., M. Chew, G. Nneji, C. Neal, J. Barry, and C. Michel. Quasi-periodic substructure in the microvessel endothelial glycocalyx: a possible explanation for molecular filtering? *J. Struct. Biol.* 136:239–255, 2001.
[145]Starling, E. H. On the absorption of fluids from the connective tissue spaces. *J. Physiol.* 19:312–326, 1896.
[146]Stevens, A. P., V. Hlady, and R. O. Dull. Fluorescence correlation spectroscopy can probe albumin dynamics inside lung endothelial glycocalyx. *Am. J. Physiol. Lung Cell. Mol. Physiol.* 293:L328–L335, 2007.
[147]Su, M., H. Jiang, P. Zhang, Y. Liu, E. Wang, A. Hsu, and H. Yokota. Knee-loading modality drives molecular transport in mouse femur. *Ann. Biomed. Eng.* 34:1600–1606, 2006.
[148]Tami, A. E., M. B. Schaffler, and M. L. Knothe Tate. Probing the tissue to subcellular level structure underlying bone's molecular sieving function. *Biorheology* 40:577–590, 2003.
[149]Tan, S. D., A. D. Bakker, C. M. Semeins, A. M. Kuijpers-Jagtman, and J. Klein-Nulend. Inhibition of osteocyte apoptosis by fluid flow is mediated by nitric oxide. *Biochem. Biophys. Res. Commun.* 369:1150–1154, 2008.
[150]Tan, S. D., T. J. de Vries, A. M. Kuijpers-Jagtman, C. M. Semeins, V. Everts, and J. Klein-Nulend. Osteocytes subjected to fluid flow inhibit osteoclast formation and bone resorption. *Bone* 41:745–751, 2007.
[151]Tan, S. D., A. M. Kuijpers-Jagtman, C. M. Semeins, A. L. Bronckers, J. C. Maltha, J. W. Von den Hoff, V. Everts, and J. Klein-Nulend. Fluid shear stress inhibits TNFalpha-induced osteocyte apoptosis. *J. Dent. Res.* 85:905–909, 2006.
[152]Tanaka, T., and A. Sakano. Differences in permeability of microperoxidase and horseradish peroxidase into the alveolar bone of developing rats. *J. Dent. Res.* 64:870–876, 1985.
[153]Tarbell, J. M. Shear stress and the endothelial transport barrier. *Cardiovasc. Res.* 87:320–330, 2010.
[154]Tarbell, J. M., and E. E. Ebong. Endothelial glycocalyx structure and role in mechanotransduction. In: Hemodynamics and Mechanobiology of Endothelium, edited by T. K. Hsiai, B. Blackman, and H. Jo. Singpore: World Scientific Publishing Co. Pte. Ltd., 2010, pp. 69–95.
[155]Tarbell, J. M., and M. Y. Pahakis. Mechanotransduction and the glycocalyx. *J. Intern. Med.* 259:339–350, 2006.
[156]Temiyasathit, S., and C. R. Jacobs. Osteocyte primary cilium and its role in bone mechanotransduction. *Ann. N. Y. Acad. Sci.* 1192:422–428, 2010.

[157]Thi, M. M., T. Kojima, S. C. Cowin, S. Weinbaum, and D. C. Spray. Fluid shear stress remodels expression and function of junctional proteins in cultured bone cells. *Am. J. Physiol. Cell Physiol.* 284:C389–C403, 2003.
[158]Thi, M. M., S. O. Suadicani, and D. C. Spray. Fluid flow-induced soluble vascular endothelial growth factor isoforms regulate actin adaptation in osteoblasts. *J. Biol. Chem.* 285:30931–30941, 2010.
[159]Thi, M. M., J. M. Tarbell, S. Weinbaum, and D. C. Spray. The role of the glycocalyx in reorganization of the actin cytoskeleton under fluid shear stress: a "bumper-car" model. *Proc. Natl Acad. Sci. USA* 101:16483–16488, 2004.
[160]Uematsu, M., Y. Ohara, J. P. Navas, K. Nishida, T. J. Murphy, R. W. Alexander, R. M. Nerem, and D. G. Harrison. Regulation of endothelial cell nitric oxide synthase mRNA expression by shear stress. *Am. J. Physiol.* 269:C1371–C1378, 1995.
[161]van den Berg, B. M., H. Vink, and J. A. Spaan. The endothelial glycocalyx protects against myocardial edema. *Circ. Res.* 92:592–594, 2003.
[162]Vezeridis, P. S., C. M. Semeins, Q. Chen, and J. Klein-Nulend. Osteocytes subjected to pulsating fluid flow regulate osteoblast proliferation and differentiation. *Biochem. Biophys. Res. Commun.* 348:1082–1088, 2006.
[163]Vink, H., and B. R. Duling. Identification of distinct luminal domains for macromolecules, erythrocytes, and leukocytes within mammalian capillaries. *Circ. Res.* 79:581–589, 1996.
[164]Visscher, K., and S. M. Block. Versatile optical traps with feedback control. *Methods Enzymol.* 298:460–489, 1998.
[165]Wang, Y., E. L. Botvinick, Y. Zhao, M. W. Berns, S. Usami, R. Y. Tsien, and S. Chien. Visualizing the mechanical activation of Src. *Nature* 434:1040–1045, 2005.
[166]Wang, L., C. Ciani, S. B. Doty, and S. P. Fritton. Delineating bone's interstitial fluid pathway in vivo. *Bone* 34:499–509, 2004.
[167]Wang, L., S. P. Fritton, S. Weinbaum, and S. C. Cowin. On bone adaptation due to venous stasis. *J. Biomech.* 36:1439–1451, 2003.
[168]Wang, N., H. Miao, Y. S. Li, P. Zhang, J. H. Haga, Y. Hu, A. Young, S. Yuan, P. Nguyen, C. C. Wu, and S. Chien. Shear stress regulation of Kruppel-like factor 2 expression is flow pattern-specific. *Biochem. Biophys. Res. Commun.* 341:1244–1251, 2006.
[169]Wang, L. Y., Y. L. Wang, Y. F. Han, S. C. Henderson, R. J. Majeska, S. Weinbaum, and M. B. Schaffler. In situ measurement of solute transport in the bone lacunar-canalicular system. *Proc. Natl Acad. Sci. USA* 102:11911–11916, 2005.
[170]Wang, Y., L. M. McNamara, M. B. Schaffler, and S. Weinbaum. A model for the role of integrins in flow induced mechanotransduction in osteocytes. *Proc. Natl Acad. Sci. USA* 104:15941–15946, 2007.
[171]Weinbaum, S. 1997 Whitaker distinguished lecture: models to solve mysteries in biomechanics at the cellular level; a new view of fiber matrix layers. *Ann. Biomed. Eng.* 26:627–643, 1998.
[172]Weinbaum, S., S. C. Cowin, and Y. Zeng. A model for the excitation of osteocytes by mechanical loading-induced bone fluid shear stresses. *J. Biomech.* 27:339–360, 1994.
[173]Weinbaum, S., Y. Duan, L. M. Satlin, T. Wang, and A. M. Weinstein. Mechanotransduction in the renal tubule. *Am. J. Physiol. Renal Physiol.* 299:F1220–F1236, 2010.
[174]Weinbaum, S., P. Guo, and L. You. A new view of mechanotransduction and strain amplification in cells with microvilli and cell processes. *Biorheology* 38:119–142, 2001.
[175]Weinbaum, S., J. M. Tarbell, and E. R. Damiano. The structure and function of the endothelial glycocalyx layer. *Annu. Rev. Biomed. Eng.* 9:121–167, 2007.
[176]Weinbaum, S., X. Zhang, Y. Han, H. Vink, and S. C. Cowin. Mechanotransduction and flow across the endothelial glycocalyx. *Proc. Natl Acad. Sci. USA* 100:7988–7995, 2003.
[177]Weinstein, A. M., S. Weinbaum, Y. Duan, Z. Du, Q. Yan, and T. Wang. Flow-dependent transport in a mathematical model of rat proximal tubule. *Am. J. Physiol. Renal Physiol.* 292:F1164–F1181, 2007.
[178]Wu, D., P. Ganatos, D. C. Spray, and S. Weinbaum. On the electrophysiological response of bone cells using a Stokesian fluid stimulus probe for delivery of quantifiable localized picoNewton level forces. *J. Biomech.* 44:1707–1708, 2011.
[179]Yao, Y., A. Rabodzey, and C. F. Dewey, Jr. Glycocalyx modulates the motility and proliferative response of vascular endothelium to fluid shear stress. *Am. J. Physiol. Heart Circ. Physiol.* 293:H1023–H1030, 2007.
[180]You, L. D., S. C. Cowin, M. B. Schaffler, and S. Weinbaum. A model for strain amplification in the actin cytoskeleton of osteocytes due to fluid drag on pericellular matrix. *J. Biomech.* 34:1375–1386, 2001.
[181]You, L. D., S. Temiyasathit, P. Lee, C. H. Kim, P. Tummala, W. Yao, W. Kingery, A. M. Malone, R. Y. Kwon, and C. R. Jacobs. Osteocytes as mechanosensors in the inhibition of bone resorption due to mechanical loading. *Bone* 42:172–179, 2008.
[182]You, L. D., S. Temiyasathit, E. Tao, F. Prinz, and C. R. Jacobs. 3D microfluidic approach to mechanical stimulation of osteocyte processes. *Cel. Mol. Bioeng.* 1:103–107, 2008.
[183]You, L. D., S. Weinbaum, S. C. Cowin, and M. B. Schaffler. Ultrastructure of the osteocyte process and its pericellular matrix. *Anat. Rec.* 278A:505–513, 2004.
[184]You, J., C. E. Yellowley, H. J. Donahue, Y. Zhang, Q. Chen, and C. R. Jacobs. Substrate deformation levels associated with routine physical activity are less stimulatory to bone cells relative to loading-induced oscillatory fluid flow. *J. Biomech. Eng.* 122:387–393, 2000.
[185]Zhang, X., R. H. Adamson, F. R. Curry, and S. Weinbaum. A 1-D model to explore the effects of tissue loading and tissue concentration gradients in the revised Starling principle. *Am. J. Physiol. Heart Circ. Physiol.* 291:H2950–H2964, 2006.
[186]Zhang, X., F. R. Curry, and S. Weinbaum. Mechanism of osmotic flow in a periodic fiber array. *Am. J. Physiol. Heart Circ. Physiol.* 290:H844–H852, 2006.
[187]Zhao, Y., S. Chien, and S. Weinbaum. Dynamic contact forces on leukocyte microvilli and their penetration of the endothelial glycocalyx. *Biophys. J.* 80:1124–1140, 2001.
[188]Zhao, H., H. Shiue, S. Palkon, Y. Wang, P. Cullinan, J. K. Burkhardt, M. W. Musch, E. B. Chang, and J. R. Turner. Ezrin regulates NHE3 translocation and activation after Na^+-glucose cotransport. *Proc. Natl Acad. Sci. USA* 101:9485–9490, 2004.